Thermochimica Acta, 193 (1991) 299–347
Elsevier Science Publishers B.V., Amsterdam

Biological calorimetry: membranes

Alfred Blume

Fachbereich Chemie der Universität Kaiserslautern, Erwin-Schrödinger-Strasse, D-6750 Kaiserslautern (Germany)

INTRODUCTION

Thermotropic phase behaviour of lipids

Besides proteins, lipids are the major constituents of biological membranes. Due to their amphiphilic nature, natural as well as synthetic lipids, when brought into contact with water, do not dissolve but spontaneously associate into aggregates, in which the contact of water with the hydrophobic chains is minimized. The hydrated lamellar phases or lipid bilayers formed spontaneously by most lipids are the essential feature, namely the permeability barrier, of biological membranes. Lipid bilayers thus serve as models for biological membranes and have therefore been the subject of intensive research over the last 20–25 years (for general reviews of lipid and membrane properties see refs. 1–3). One of the major classes of lipids occurring in membranes are the phospholipids. The general formula for phospholipids is shown in Fig. 1 (left). Phospholipids are diesters of *sn*-glycero-3-phosphoric acid. The fatty acyl residues at the *sn*-1 and *sn*-2 position of the glycerol vary in length (14–24 carbon atoms) and degree of unsaturation (1–4 double bonds). In natural phospholipids generally, two different fatty acids are esterified to the glycerol OH groups. The phosphate group usually carries a second short alcohol (group X) as a substituent, as shown in Fig. 1. Depending on the chemical nature of this substituent, the phospholipid is either zwitterionic or negatively charged at neutral pH. Figure 1 (right) shows a variety of phospholipids with identical palmitoyl chains but with different polar groups as they occur in biological membranes. The usual abbreviations for the different phospholipid classes are given; the first two letters stand for the fatty acyl chains (in this case DP for dipalmitoyl) and the last two letters for the head group (for instance PC for phosphatidylcholine) as indicated in the figure legend.

Phospholipids show thermotropic and lyotropic phase behaviour. When dispersed in excess water these lipids form hydrated bimolecular lamellar phases, in which the lipid molecules are packed either in a quasi-crystalline two-dimensional lattice, the so-called gel phase, or remain in a lamellar arrangement but show higher two-dimensional fluidity. This is the liquid-

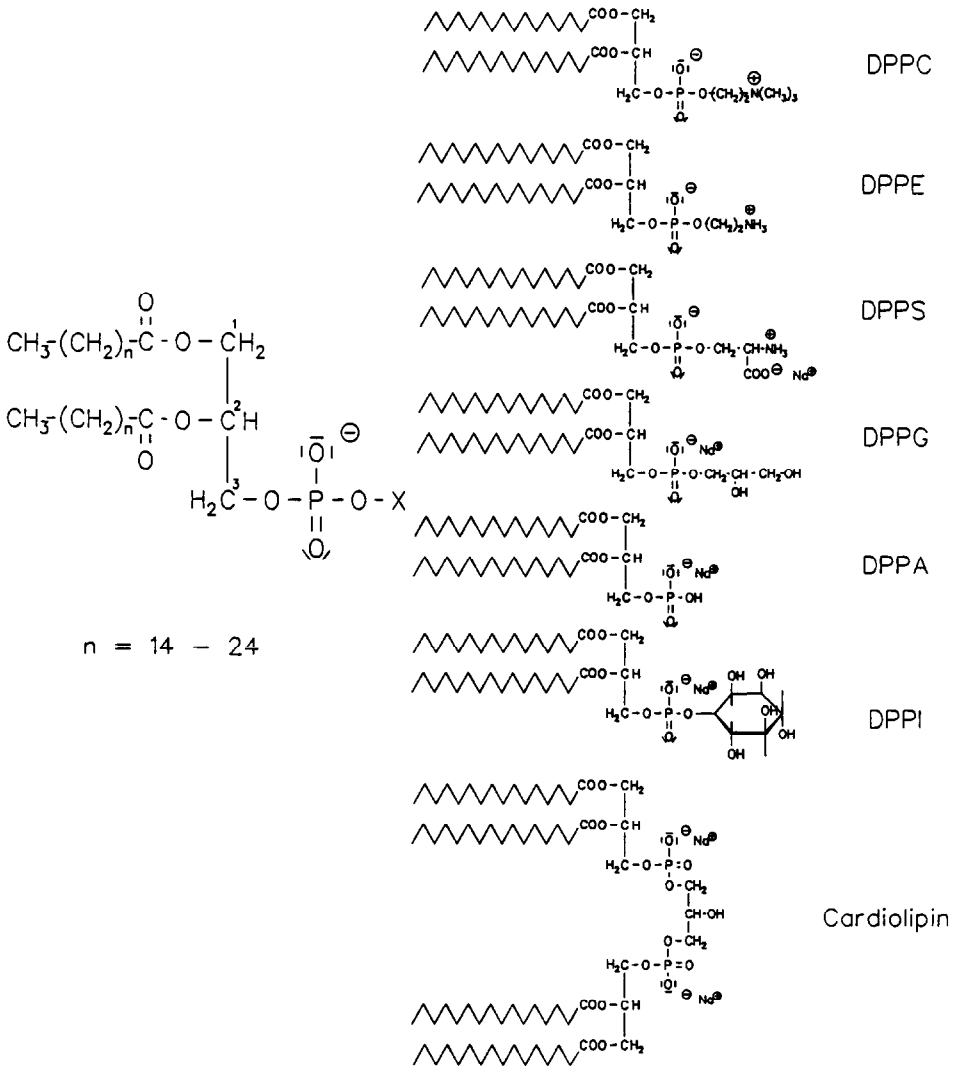

Fig. 1. Left: chemical structure of phospholipids with saturated fatty acyl chains. X = variable group. Right: chemical structures of phospholipids with two palmitoyl chains. Abbreviations:
1,2-dipalmitoyl-*sn*-glycero-3-phosphocholine (DPPC);
1,2-dipalmitoyl-*sn*-glycero-3-phosphoethanolamine (DPPE);
1,2-dipalmitoyl-*sn*-glycero-3-phosphoserine (DPPS);
1,2-dipalmitoyl-*sn*-glycero-3-phosphoglycerol (DPPG);
1,2-dipalmitoyl-*sn*-glycero-3-phosphatidic acid (DPPA);
1,2-dipalmitoyl-*sn*-glycero-3-phosphoinositol (DPPI);
1′,3′-di-*O*-(1,2-dipalmitoyl-*sn*-glycero-3-phospho)glycerol (Cardiolipin).

crystalline phase. Depending on the chemical structure either one of these phases is the stable one at room temperature. Transitions between these phases can be induced by temperature changes, changes in hydration, pH changes or binding of cations. In Fig. 2 two representative cases for the

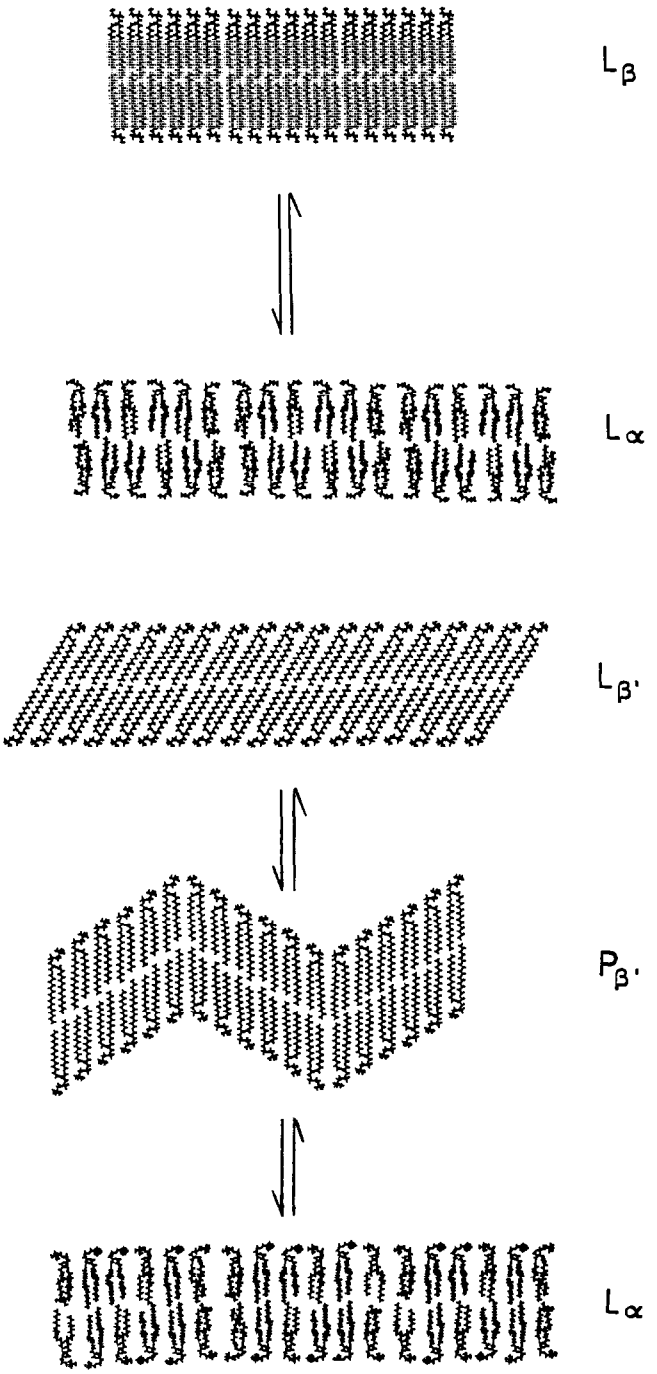

Fig. 2. Schematic drawing of the phase transitions between lamellar phases taking place in excess water for PEs (top) and PCs (bottom).

phase changes occurring in phospholipid bilayers are shown. Figure 2 (top) shows the phase behaviour of phosphatidylethanolamines (PEs) in excess water. PEs with identical saturated fatty acyl chains show a particularly simple thermotropic behaviour as only one major phase transition is observed from the lamellar L_β phase (gel phase) to the lamellar L_α phase (liquid-crystalline or l.c. phase). In the l.c. phase there is high mobility of the molecules in the plane of the bilayer and the acyl chains are "fluid" in the sense that they display increased trans–gauche isomerization. In the gel phase the acyl chains are packed in an almost all-trans conformation in a hexagonal lattice. Lateral diffusion is greatly inhibited.

Phosphatidylcholines (PCs) with saturated identical fatty acyl chains show a more complicated phase behaviour as at least two different gel phases are observed, a so-called intermediate $P_{\beta'}$ phase, in which the surface of the bilayer is distorted by a periodic ripple, which is either sinusoidal or more probably saw-tooth like, and at lower temperature an $L_{\beta'}$ phase in which the molecules are tilted at an angle of about 30° relative to the bilayer normal. When PC dispersions are cooled for extended periods of time (hours to days) at temperatures just above 0 °C, a fourth lamellar phase is formed, the so-called L_c phase, in which the chains are highly ordered in an orthorhombic lattice. The L_c to $L_{\beta'}$ transition has been termed sub-transition. At low hydration levels transition temperatures between the different phases usually increase and other structures and phase sequences can be observed. Figure 3 shows a phase diagram for the lipid 1,2-dipalmitoyl-*sn*-glycero-3-phosphocholine (DPPC) with the corresponding sketches for the chain packing modes [3]. The inset shows a comparison of phase diagrams for PCs with other chain lengths.

Differential scanning calorimetry (DSC) has been one of the most widely used methods for studying the thermal behaviour of hydrated lipid bilayer membranes since the pioneering work of Chapman and coworkers [4–8]. Since then numerous review articles describing the thermotropic behaviour of membranes, lipid bilayers and lipid–protein membranes have appeared and thermotropic data as determined by DSC have been compiled [3,9–24].

In this article a comprehensive review of thermal data of lipid membranes will not be attempted, but the focus will be on selected examples for the application of calorimetric methods in membrane research. As no review is intended most of the examples shown are from recent work of the author's own group. References to similar or related work by other groups will be given but they will by no means be complete for the reasons mentioned above, so the huge amount of work done by numerous other groups will necessarily be misrepresented. To gain more information the reader is referred to the reviews cited above.

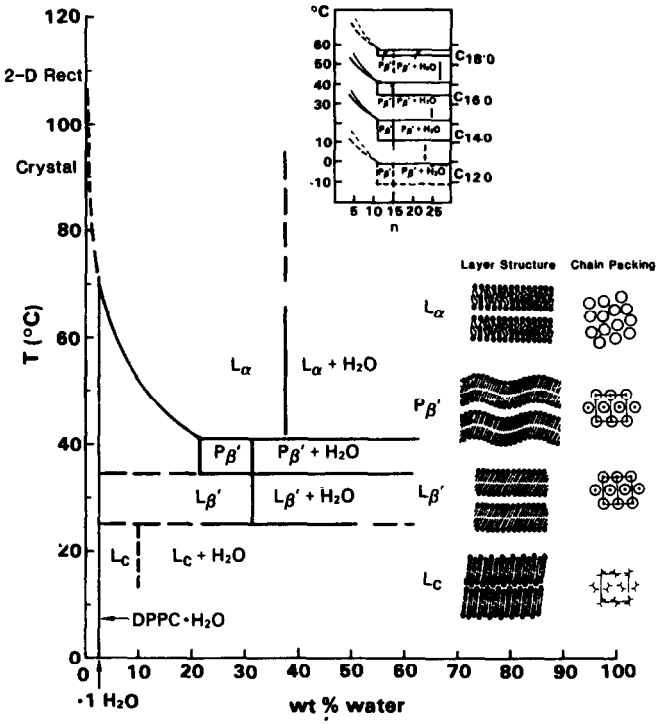

Fig. 3. Phase diagram for PC/water systems (from ref. 3).

DIFFERENTIAL SCANNING CALORIMETRY OF LIPID MEMBRANES

Models for the phase transition of lipids

For the description of the lipid phase transition a simple two-state model assuming an equilibrium between state A (gel) and B (l.c.) is often assumed and is also sufficient to understand the basic thermodynamic properties of the lipid phase transition. For an equilibrium between two states

$$A \rightleftharpoons B \tag{1}$$

the equilibrium constant K can be expressed using the degree of transition Θ

$$K = \frac{[B]}{[A]} = \frac{\Theta}{1-\Theta} \tag{2}$$

with

$$\Theta = \frac{K}{1+K} \tag{3}$$

ranging between 0 (gel phase) and 1 (l.c. phase).

The temperature dependence of K is described by the van't Hoff equation

$$K(T) = K(T_m)\ \exp[-\Delta H_{vH}/R(1/T - 1/T_m)] \tag{4}$$

with T_m being the midpoint of the transition at the temperature where $\Theta = 0.5$ and with $K(T_m) = 1$.

In a DSC experiment one measures the differential heat capacity c_{diff} as a function of temperature. c_{diff} is related to the total transition enthalpy Δh_{cal} and the temperature dependence of Θ by

$$c_{diff} = \Delta h_{cal}(d\Theta/dT) \tag{5}$$

Calculating $d\Theta/dT$ from eqns. (2) and (3) and inserting into eqn. (4) yields

$$c_{diff} = \Delta h_{cal}\left\{\frac{\exp[(-\Delta H_{vH}/R)(1/T - 1/T_m)]\ \Delta H_{vH}/RT^2}{(1 + \exp[(-\Delta H_{vH}/R)(1/T - 1/T_m)])^2}\right\} \tag{6}$$

The value of Δh_{cal} is determined from the experimental DSC curve by integration over the DSC peak from T_{onset} where the deviation from the base line starts to T_{end} where the signal returns to the base line

$$\int_{T_{onset}}^{T_{end}} c_{diff}\ dT = \Delta h_{cal} \tag{7}$$

Δh_{cal} can be converted to the molar transition enthalpy ΔH_{cal} from the known amount of material. Figure 4 shows a calculated curve according to eqn. (6) using three different values for the van't Hoff transition enthalpy

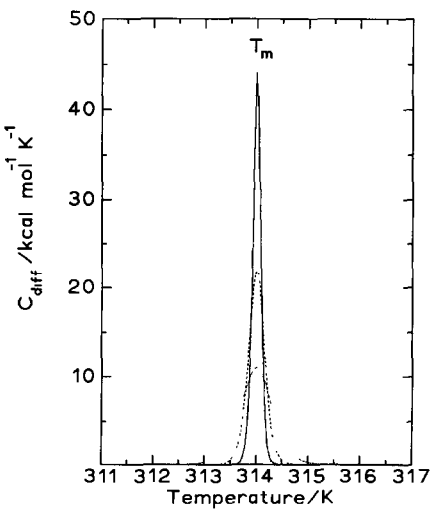

Fig. 4. Calculated transition curves for a two-state transition according to eqn. (6) with $T_m = 314$ K, $\Delta H_{cal} = 8.7$ kcal mol^{-1} and $\Delta H_{vH} = 4000$, 2000, and 1000 kcal mol^{-1}, corresponding to cooperative unit sizes of 460, 230, and 115 molecules.

ΔH_{vH}. The calorimetric transition enthalpy ΔH_{cal} is much lower than the transition enthalpy ΔH_{vH}, which can be calculated from the van't Hoff equation (eqn. 4) under the assumption of a true equilibrium between states A and B. The ratio $\Delta H_{vH}/\Delta H_{cal}$ is unity for a true equilibrium and goes to infinity for a melting process of an ideal crystal. For cooperative transitions, such as the lipid phase transition the ratio $\Delta H_{vH}/\Delta H_{cal}$ is called the cooperative unit (c.u.) and is thus a measure of the degree of cooperativity between lipid molecules [25,26].

To determine c.u. ΔH_{vH} has to be known. This can easily be calculated from the same calorimetric experiment using eqn. (6) at $T = T_m$ for which $\Theta = 0.5$

$$(d\Theta/dT)_{T_m} = \Delta H_{vH}/4RT_m^2 \tag{8}$$

$$\Delta H_{vH} = 4RT_m^2(d\Theta/dT)_{T_m} = \frac{4RT^2C_{max}}{\Delta H_{cal}} \tag{9}$$

Thus ΔH_{vH} can either be calculated from the slope of the integrated DSC curve at $\Theta = 0.5$ or from the maximum in the c_{diff} curve C_{max} at T_m, where C_{max} has to be expressed in molar units. Typical values for c.u. determined for phase transitions of pure lipids vary roughly between 20 and 2000, depending on the purity of the sample and the chemical structure of the lipid. The determination of large c.u. is experimentally difficult due to instrumental broadening effects when the transitions are very sharp. Theoretically this can be removed by deconvolution once the apparatus function is known. In practice very slow scan speeds are usually applied, taking into account the decreased sensitivity of the instruments under these conditions. All these equations are only valid for the simple symmetric two-state process. In reality the experimental DSC curves show in many cases that the transitions are not symmetric as shown in Fig. 4, but asymmetric with a broader shoulder on the low temperature side.

Numerous models exist for theoretical descriptions of lipid phase transitions in two-dimensional systems. We will not discuss these theories here but refer to recent reviews [27,28].

Phase transition of pure phospholipids

For DSC studies of lipid systems and natural membranes high sensitivity is essential and therefore DSC instruments of the adiabatic type are to be preferred. Basically two calorimeters of this type have gained widespread acceptance, namely the DASM-1M and its successor DASM-4M (Mashpriborintorg, Moscow, USSR) designed by Privalov [29] and the Microcal MC 2 (Microcal Inc., Amherst, MA, USA), which is essentially similar in cell design to the DASM-1M. Several other types of DSC instruments, mainly of the heat conduction type were also used in the

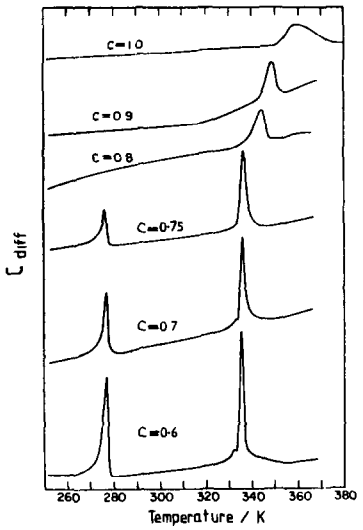

Fig. 5. DSC curves of DSPC as a function of water content C (from ref. 5).

beginning and are still useful when the hydration dependence of lipid phase behaviour at low water content is investigated, where the adiabatic DSC instruments cannot be used, due to their much larger cell volumes.

Anhydrous phospholipids such as phosphatidylcholines show thermotropic mesomorphism, i.e. several phase changes occur below the capillary melting point [4]. Phospholipids also exhibit lyotropic mesomorphism, their phase states changing upon addition of water (see Fig. 3). Figure 5 shows as a classical example DSC curves of DSPC as a function of water content as recorded by Chapman and co-workers [5]. Increasing amounts of water shift the transition peak to lower temperature, the transition also becoming sharper. Addition of excess water leads to the appearance of an extra peak at 0 °C due to the melting of excess water. A considerable amount of water is "bound" to the head group and does not freeze at 0 °C. As is evident from Fig. 5, about 30% of the total water content does not freeze. This behaviour is similar for all PCs with different saturated fatty acyl chains as indicated in the inset of Fig. 3.

As all biological membranes are in excess water we will focus from now on only on lipid bilayers and membranes at high water content, and will not discuss the various phases appearing at low hydration. In addition we will restrict the presentation of examples for lipid behaviour to results on the phase transitions of phospholipids between different lamellar phases and will not describe DSC studies of the lamellar to hexagonal phase transition or of other lipid classes like sphingolipids and glyceroglycolipids.

The lyotropic behaviour of phospholipids depends on the nature of the lipid head group as mentioned before and as shown in Figs. 1 and 2. Figure 6 shows DSC scans of three PCs and three PEs with different chain lengths

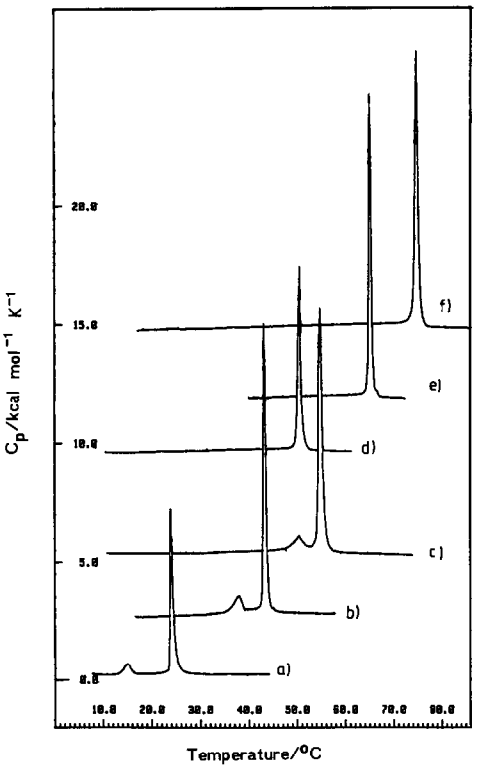

Fig. 6. DSC curves of (a) DMPC, (b) DPPC, (c) DSPC, (d) DMPE, (e) DPPE, (f) DSPE (from ref. 117a).

to illustrate both the effects of increasing the length of the acyl chains and the effects of changing the chemical structure of the head group. For PCs two transitions, the pre-transition to the $P_{\beta'}$ phase and the main transition are clearly discernible. PEs show only one transition to the liquid-crystalline phase. The sub-transition for PCs, which was discussed above, is not shown in these traces. This transition only develops after prolonged storage at low temperature, the transition enthalpy and temperature depending strongly on the incubation times [30,31].

The transition temperatures of PEs are markedly higher than those of PCs. This is due to strong intermolecular hydrogen bonding between the head groups and lower hydration numbers [1,22]. The L_β phase of PEs was shown to be metastable [32]. After longer incubation the L_β phase of DLPE, for instance, reverts to an L_c phase, which then transforms to the liquid-crystalline phase at higher temperature, namely 35 °C. Incubation of the L_α phase of DLPE at a temperature just below 40 °C leads to the formation of a dehydrated $L_{c'}$ phase, which transforms to the L_α phase at even higher temperature, namely 42 °C. For longer chain PEs these incubation times increase; they are dependent on the water content of the sample and the chain length of the PE [32].

TABLE 1

Transition temperatures T_m, transition enthalpies ΔH_{cal} and transition entropies ΔS_{cal} for the pre-transition (index 1) and main transition (index 2) of phospholipids with identical saturated fatty acyl chains in dilute aqueous dispersion; numbers designate length of acyl chain *n*

Lipid	*n*	T_{m1} (°C)	ΔH_{cal1} (kcal mol^{-1})	T_{m2} (°C)	ΔH_{cal2} (kcal mol^{-1})	ΔS_{cal2} (cal mol^{-1} K^{-1})	Ref.
PC	12:0			−2.1	1.8	6.6	31
	13:0	−0.8	0.5	13.7	4.4	15.3	31
	14:0	15.3	1.3	24.0	6.5	21.9	23,109
		14.3	1.1	23.9	5.9	19.9	31
	15:0	24.8	0.9	34.7	6.9	22.4	31
	16:0	35.5	1.6	41.5	8.7	27.7	23,109
		34.2	1.1	41.4	7.7	24.5	31
	17:0	43.0	1.1	49.8	8.7	27.0	31
	18:0	51.0	1.8	54.3	10.9	33.3	23,109
		50.7	1.2	55.3	9.8	29.9	31
	19:0	57.8	1.3	61.8	10.7	32.0	31
	20:0	62.1	1.7	64.1	12.3	37.6	23,109
		63.7	1.4	66.4	11.4	33.6	31
	21:0	68.7	1.4	71.1	12.2	35.5	31
	22:0			72.5	14.9 [a]	43.1	23,109
				74.8	14.9 [a]	42.8	31
PE	12:0			30.5	4.3	14.2	23,109
				30.5	3.7	12.2	44
	14:0			49.9	6.6	20.4	23,109
				49.5	5.7	17.8	44
	16:0			63.9	8.6	25.5	23,109
				64.0	7.9	23.4	44
	17:0			70.5			42
	18:0			74.1	10.9	31.4	117
				74.0	10.5	30.3	44
				74.2			42
	19:0			79.2			42
	20:0			81.1	12.2	34.5	23,109
				82.5	12.5	35.3	44
				83.1			42
PA [b]	12:0			33.5	3.4	11.1	23,109
[c]				32.0	3.3	11.0	1
[b]	14:0			52.2	5.7	17.5	21,109
[c]				50.0	5.5	17.0	1
[b]	16:0			65.0	7.9	23.4	23,109
[c]				68.0	7.9	23.1	1
PG [c]	12:0			−2.0			1
[b]	14:0			26.0	7.1	25.4	119
[c]				24.0	6.8	22.9	1
[b]	16:0			43.5	10.0	31.6	119
[c]				41.4	8.8	28.0	1
[b]	18:0			57.0	13.0	39.4	119
[c]				54.5	10.5	32.1	1

TABLE 1 (continued)

Lipid	n	T_{m1} (°C)	ΔH_{cal1} (kcal mol^{-1})	T_{m2} (°C)	ΔH_{cal2} (kcal mol^{-1})	ΔS_{cal2} (cal mol^{-1} K^{-1})	Ref.
PS [c]	12:0			13.0	3.1	10.9	1
[c]	14:0			36.0	6.9	22.4	1
[c]	16:0			52.0	8.8	27.2	1
[c]	18:0			68.0	11.0	32.2	1

[a] ΔH_{cal2} value is sum of pre- and main transition.
[b] In pure water at about 2.5 mM concentration.
[c] Ionic strength $I = 0.1$ M.

The calorimetric transition enthalpies ΔH_{cal} can be determined by integration from the DSC peaks and the transition entropies ΔS can then be calculated from $\Delta H_{cal}/T_m$ as $\Delta G = 0$ at $T = T_m$. Table 1 summarizes thermodynamic data for a variety of phospholipids with identical saturated fatty acids but different head groups. Figure 7 shows a plot of the transition temperatures versus chain length. This plot is clearly non-linear and shows that for lipids with longer chains the effects of different head group structure decrease. The plots of ΔH_{cal} versus chain length shown in Fig. 8 for PCs and PEs are essentially linear for chain lengths larger than 14 carbon atoms. The slope of the linear regression line through the data points for PCs is between 0.98 and 0.92 depending on the data reported by different groups. Thus ΔH_{cal} increases by about 0.46–0.49 kcal mol^{-1} per additional CH_2 group in the chain. For PEs the slope of ΔH_{cal} versus chain length is similar. For PEs a value of 0.5 kcal mol^{-1} per CH_2 group is

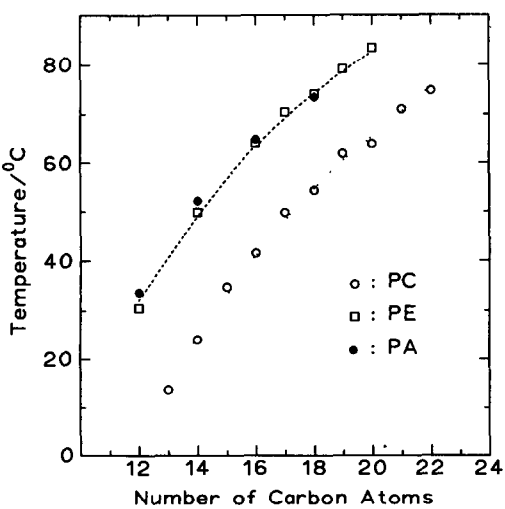

Fig. 7. Dependence of transition temperature T_m on chain length for PCs, PEs and PAs (data from refs. 23, 31, 44, 63, 109).

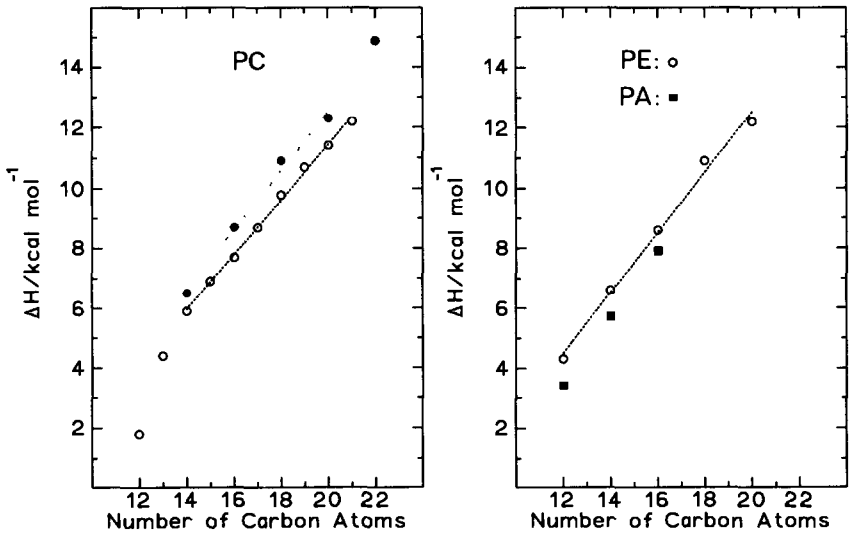

Fig. 8. Dependence of transition enthalpy ΔH_{cal} on chain length (PCs, o (from ref. 31); •, (from ref. 109). PE, o; and PA, ■ (from refs. 44, 63, 109, 117)).

obtained. Because of the higher T_m values of PEs the transition entropies ΔS are slightly lower (see Table 1). This indicates that intermolecular interactions via hydrogen bonds, which are responsible for the higher T_m values of PEs, also affect the transition entropy. In the liquid-crystalline phase PEs seem to have slightly less motional freedom than PCs. This has been verified by recent ^2H NMR measurements [33,34]. Figure 8 also illustrates the characteristic variations reported for transition enthalpies of lipids in excess water as determined by different groups using different DSC instruments. Part of the differences in the reported ΔH_{cal} values may be instrument related or due to different purities of the samples. An additional reason is that the positioning of the base-line for the determination of ΔH_{cal} is not quite unambiguous, particularly for PCs where the pre-transition peaks overlap as is the case for the longer chain analogues. For instance, for DPPC the reported values for the main transition enthalpy vary between 6.9 and 9.69 kcal mol^{-1} (see ref. 3 for tabulation of data).

Introduction of double bonds into the fatty acyl chains depresses the temperature of the main transition and the pre-transition is usually absent in these compounds. The decrease in the main transition of PCs is similar to the decrease of the melting points of the fatty acids. Figure 9 shows the transition enthalpy and transition temperature of PCs with one and two *cis*-octadecenoic acid chains, where the position of the double bond was varied along the chain [35]. When the double bond is in the middle of the chain the strongest reduction in T_m is observed and also ΔH_{cal} passes

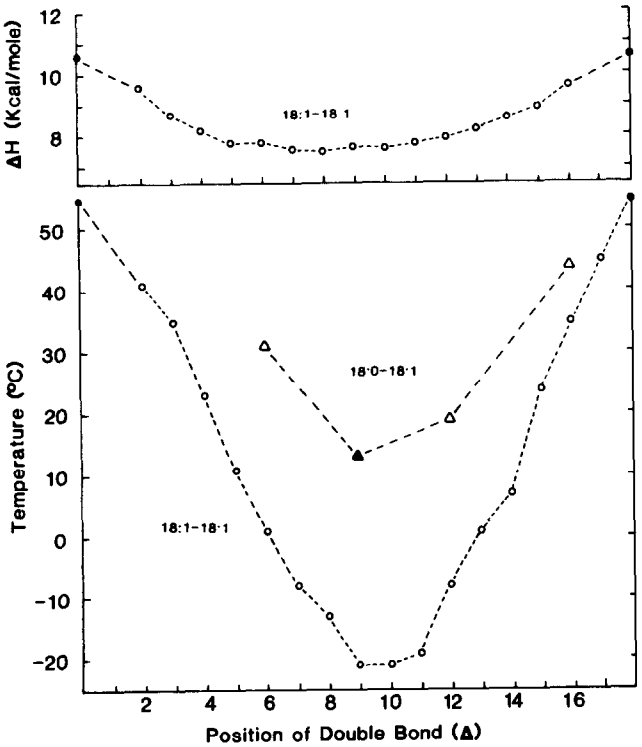

Fig. 9. Dependence of ΔH_{cal} and T_m on the position of the double bond in PCs with a chain length of 18 C atoms (from refs. 3, 35).

through a minimum. At this position the perturbation of the chain packing in the gel state is greatest.

Similar studies have recently been made with lipids containing branched chain fatty acids. Menger et al. [36] synthesized various homologues of DSPC having an additional methyl group at different positions in the chains. The position was systematically varied. Figure 10 shows how T_m and ΔH_{cal} vary as a function of the position of the methyl branch in the *sn*-2 chain of the PC.

Lewis et al. [37] have studied the thermotropic behaviour of PCs with *cis*-mono-unsaturated fatty acids of different chain length. The position of the double bond was varied between 9 for oleic acid and 15 for nervonic acid, the distance to the terminal methyl group thus staying constant. The PCs with cis-unsaturated fatty acid chains all showed a transition from a quasi-crystalline L_c phase to an L_α phase. Figure 11 shows the variation of T_m and ΔH_{cal} with chain length. Slight even–odd effects are evident from these plots. The formation of the highly ordered phase at low temperature is thus very sensitive to the position of the potentially perturbing group and also to the total chain length.

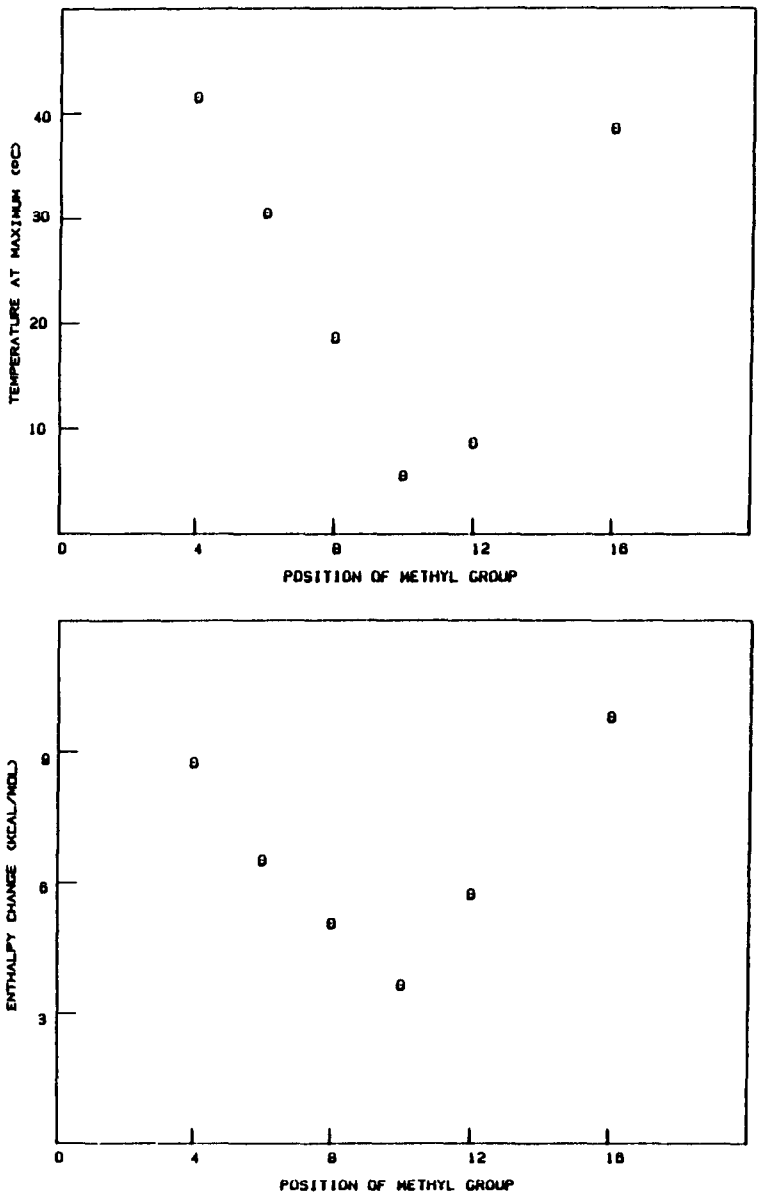

Fig. 10. Dependence of T_m and ΔH_{cal} on the position of an extra methyl group in the *sn*-2 chain of a PC with 18 C atoms in both chains (from ref. 36).

Various mixed-chain PCs with saturated fatty acids have been synthesized and investigated by DSC and other methods. Their thermotropic behaviour and lamellar structures have been reviewed in detail by Huang and Mason [20]. We will show only one recent example of these systematic studies. Figure 12 shows the DSC curves and the variation of T_m and ΔH_{cal} of PCs as a function of the length of the *sn*-1 chain and *sn*-2 chain

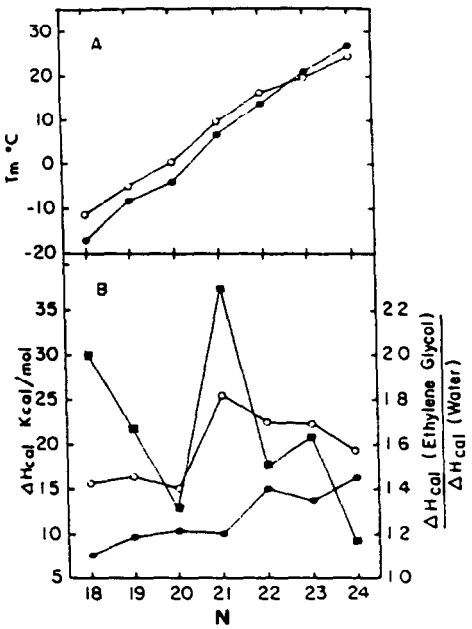

Fig. 11. (A) Dependence of T_m for PCs with cis-unsaturated chains of varying length in water (●) and (○) aqueous ethylene glycol. (B) Dependence of ΔH_{cal} for dispersions in water (●) and in aqueous ethylene glycol (○). Ratio of the transition enthalpies in aqueous ethylene glycol to transition enthalpies in water is indicated by (■) (from ref. 37).

respectively [38]. PCs with unequal chain lengths can form partly or fully interdigitated bilayers with 2 or 3 fatty acyl chains per head group as shown schematically in Fig. 13 for the case of C(8):C(18)-PC and C(10):C(18)-PC. C(8):C(18)-PC behaves identically for instance, to C(18):C(10)-PC and not to its positional isomer C(18):C(8)-PC. This is due to different conformations at the *sn*-2 chain, which has a characteristic bend at the glycerol backbone, whereas the *sn*-1 chain is straight with respect to the glycerol [39,40]. No other phospholipid class has been studied in such detail as phosphatidylcholines. A compilation of thermotropic data for PCs can be found in refs. 1 and 3.

The second phospholipid class which has been studied more systematically is that of phosphatidylethanolamines. Data for their thermotropic behaviour are included in Table 1 and Figs. 6–8. Recently PEs with fatty acyl chains other than saturated ones have also been investigated and also PEs with mixed saturated chains have been studied [41–43]. In addition to the gel to l.c. phase transition PEs can also convert to the so-called inverted hexagonal H_{II} phase in which the molecules are arranged in cylinders, the cylinders being packed in a hexagonal lattice [1,44]. The transition from the lamellar L_α phase to the H_{II} phase occurs at higher temperature than the L_β–L_α phase transition, for saturated PEs with

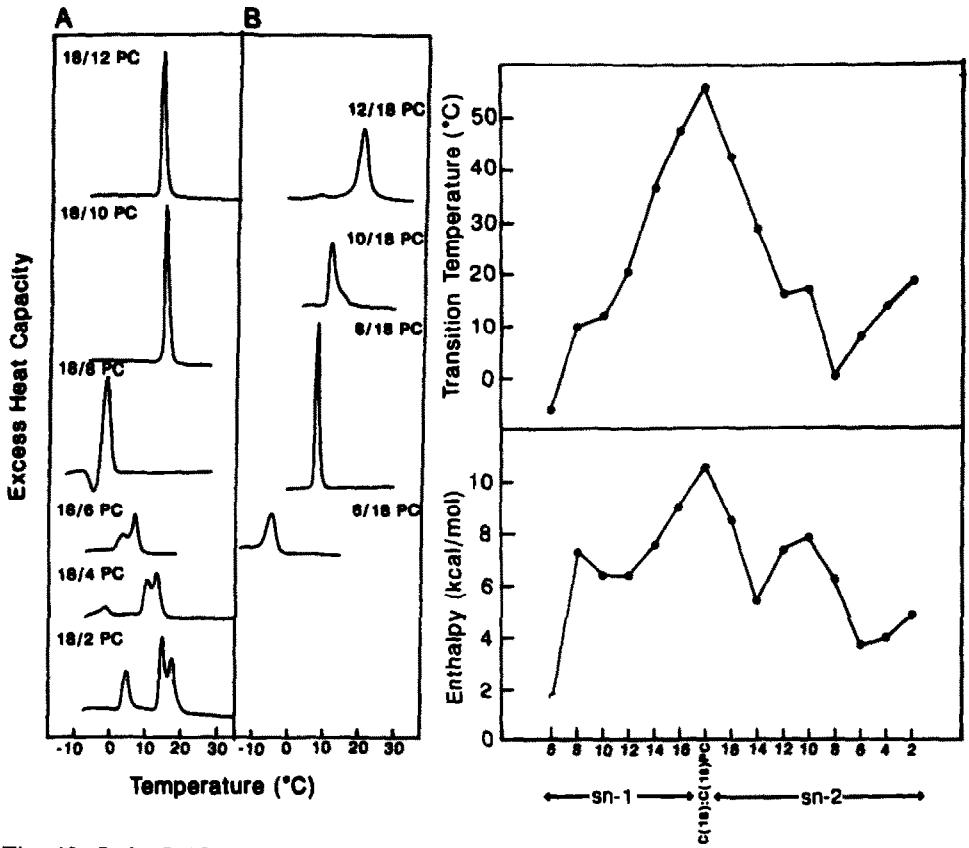

Fig. 12. Left: DSC curves of PCs with mixed acyl chains of different lengths. Right: Dependence of T_m and ΔH_{cal} on the lengths of the *sn*-1 and *sn*-2 chain (from ref. 38).

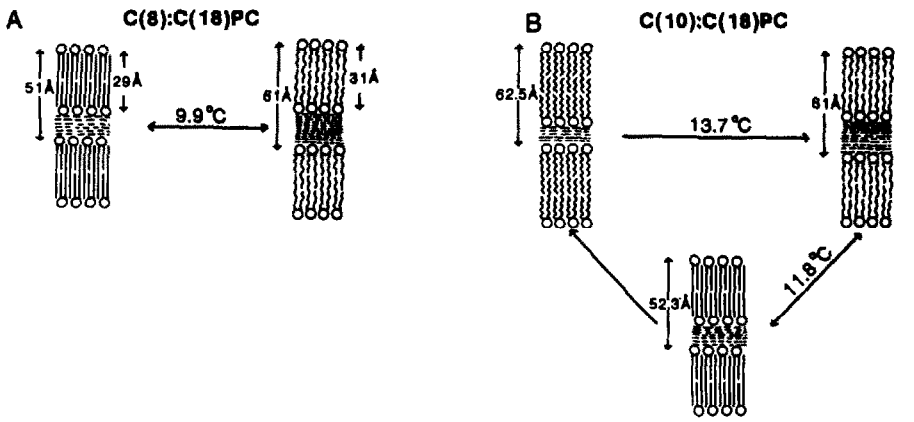

Fig. 13. Schematic drawings of the temperature dependent structural changes in fully hydrated bilayers of (A) C(8):C(18)PC and (B) C(10):C(18)PC (from ref. 38).

shorter chain lengths even above 100 ° C [42,44]. Unsaturation of the chains or methyl branching reduces the L_α–H_{II} phase transition temperature. A systematic study of these effects has been performed by Lewis et al. [42].

Phase diagrams of binary lipid mixtures

As biological membranes are a complex mixture of different lipid classes having a broad distribution of different fatty acids, the mixing behaviour of lipids in the different phase states is therefore of great interest. Deviations from ideal mixing or even limited miscibility in the gel phase can have important implications for liquid-crystalline phase behaviour. Non-ideal mixing can imply lateral inhomogeneities in the liquid-crystalline phase leading to cluster formation of like molecules [45–48]. Cluster formation in turn can influence the function of enzymes built into the membrane. The phase behaviour of binary phospholipid mixtures in two-dimensional bilayers can be treated in a similar way as the behaviour of three-dimensional systems [11,49]. Figure 14 shows schematically four principal types of phase diagram for binary mixtures which can be observed. In DSC experiments the points on the liquidus and solidus curves are determined from the temperatures at the onset and the end of melting shown by the DSC peaks. In lipid mixtures this is sometimes difficult as the transition peaks are very

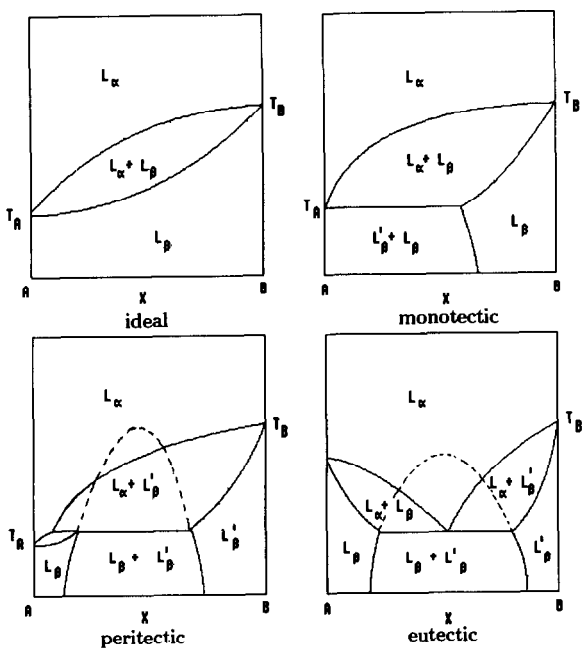

Fig. 14. Schematic drawing of possible phase diagrams for pseudo-binary mixtures of lipids in excess water.

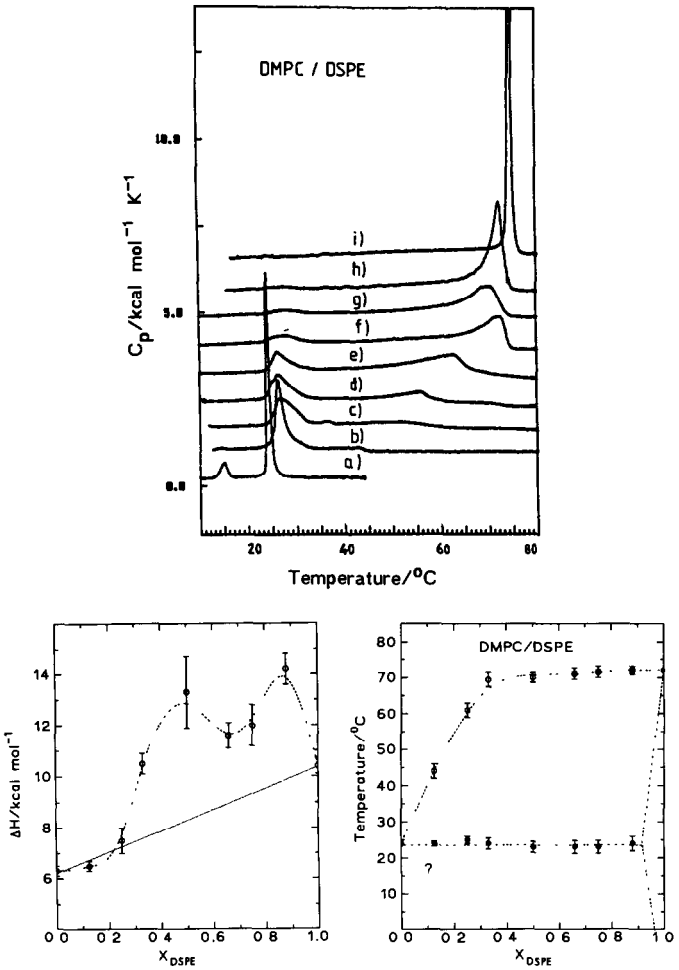

Fig. 15. Top: DSC scans of DMPC/DSPE mixtures at various compositions corresponding to the mole fractions shown in bottom figures. Bottom: (Left) Dependence of ΔH_{cal} on composition and (right) phase diagram for DMPC/DSPE obtained after correction for the finite width of the transition of the pure compounds. At low DSPE content an area is marked with a question mark where the phase diagram due to the occurrence of the $P_{\beta'}$-phase of DMPC is unclear (from refs. 46, 117a).

broad. Several extrapolation procedures have been suggested to remove the finite width of the transition due to instrumental broadening (usually negligible for these broad transitions in lipid mixtures) and broadening due to limited cooperativity, which is the main effect. The problem is illustrated by the DSC scans shown in Figs. 15 and 16 for two different PC/PE systems, the first showing DSC scans typical for systems with a miscibility gap in the gel phase and the second typical for a system with complete miscibility in both phases. For all mixtures the transitions are very broad and the onset and end of melting difficult to determine. To obtain singular

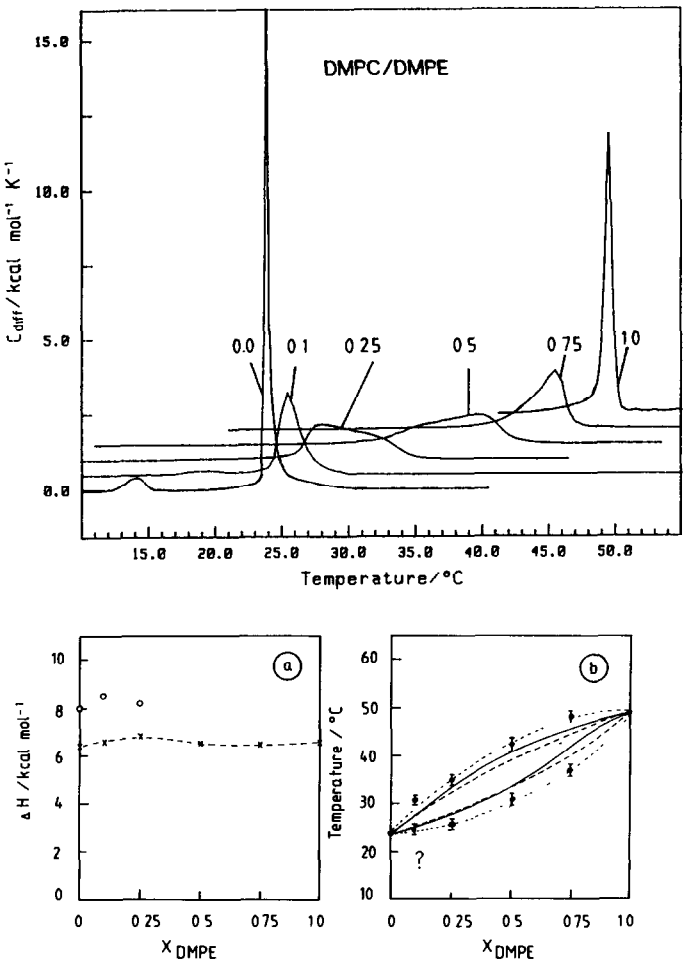

Fig. 16. Top: DSC scans of DMPC/DMPE mixtures at various mole fractions of DMPE as indicated. Bottom: (a) dependence of ΔH_{cal} on composition: ×, only the main transition; ○, with pre-transition included. (b) Phase diagram from DMPC/DMPE obtained after correction for the finite width of the transition (●) and calculated phase boundaries for ideal miscibility in both phases (broken line) and non-ideal mixing in both phases (solid line). See text and Table 2 for parameters. The region of the $P_{\beta'}$ phase of pure DMPC and DMPC/DMPE mixtures with low PE content is marked by question mark (adapted from ref. 23).

points at the position of the pure compounds in the binary phase diagram, as shown in Figs. 15 and 16, the simplest procedure for correcting the experimental values for T_{onset} and T_{end} involves subtracting the finite width of the phase transition of the pure compounds according to their mole fractions. This method was used to obtain the points in the phase diagrams of Figs. 15 and 16.

The DMPC/DSPE system in Fig. 15 is clearly of a type with a large miscibility gap in the gel phase [46]. This is due to the chain length

difference of four CH_2 groups between the two compounds and because the PE has the longer chain and a much higher transition temperature. This behaviour has been predicted theoretically by Sugar and Monticelli [50,51]. In the system DMPC/DMPE there is no chain length difference. This mixture behaves almost ideally [23,50].

Phase diagrams can be analyzed, for instance, using regular solution theory with a non-ideality parameter describing the deviations from ideal mixing [11,16,47,49]. With the help of the non-ideality parameter cluster sizes can be calculated [47,48]. Various binary lipid mixtures have been analyzed using this procedure [16,52–54] and theoretical predictions on the basis of Landau theories have been made [50,51,55]. As an example we will show here the analysis of the DMPC/DMPE phase diagram.

In regular solution theory the non-ideality of the mixture is solely attributed to the excess enthalpy of mixing, the excess entropy of mixing being zero. The non-ideality parameter is then temperature independent. We have analysed the DMPC/DMPE system using standard thermodynamics with a temperature dependent non-ideality parameter $A = a - bT$. The following equations describe the ratios of the mole fractions x_i of component 1 and 2 in the liquid-crystalline (lc) and gel (g) phases

$$\ln\left(\frac{x_1^{lc}}{x_1^{g}}\right) = \frac{\Delta H_1}{R}\left(\frac{T - T_{m1}}{T T_{m1}}\right) - \ln\left(\frac{f_1^{lc}}{f_1^{g}}\right) \tag{10}$$

and

$$\ln\left(\frac{x_2^{lc}}{x_2^{g}}\right) = \ln\left(\frac{1 - x_1^{lc}}{1 - x_1^{g}}\right) = \frac{\Delta H_2}{R}\left(\frac{T - T_{m2}}{T T_{m2}}\right) - \ln\left(\frac{f_2^{lc}}{f_2^{g}}\right) \tag{11}$$

with f_i, ΔH_i, and T_{mi} being the activity coefficients, the calorimetric transition enthalpies and transition temperatures of the two components. For the activity coefficients f_i one obtains from a series expansion of the excess Gibbs free energy of mixing, keeping only the first coefficient [56]

$$\overline{\Delta G}^{E} = x_2(1 - x_2)A \tag{12}$$

$$\ln f_1 = x_2^2 A/RT \tag{13}$$

$$\ln f_2 = (1 - x_2)^2 A/RT \tag{14}$$

If A is temperature dependent then

$$\left(\partial\, \overline{\Delta G}^{E}/\partial T\right) = -\overline{\Delta S}^{E} = (\partial A/\partial T)x_2(1 - x_2) = b x_2(1 - x_2) \tag{15}$$

For the case of $(\partial A/\partial T) = 0$ we have the so-called regular solution mentioned above with $\overline{\Delta S}^{E} = 0$ and $\overline{\Delta G}^{E} = \overline{\Delta H}^{E}$.

For the DMPC/DMPE mixture the non-ideality parameter $A = a - bT$ was not obtained directly from the points of the liquidus and solidus curves

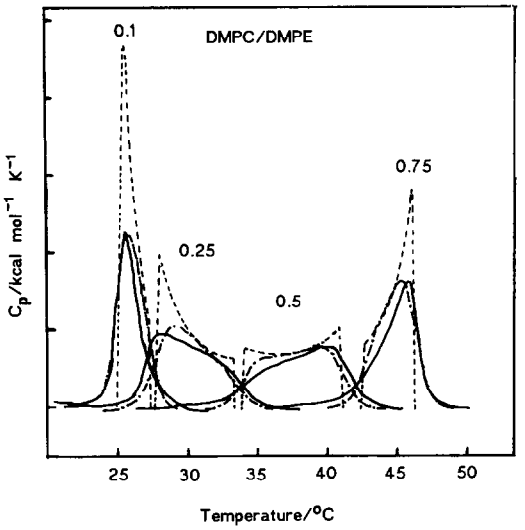

Fig. 17. Experimental DSC curves for DMPC/DMPE (solid lines), calculated curves with non-ideal mixing (broken lines) and calculated curves after convolution with a broadening function similar to eqn. (6) (broken and dotted line) (adapted from ref. 23).

of the phase diagram but rather by simulation of the experimental DSC curves. This was accomplished by calculating from the simulated phase diagram theoretical C_{diff} versus T curves. The limited cooperativity of the system was taken into account by performing a convolution of the theoretical C_{diff} curves with a broadening function which had essentially the shape of the theoretical c_{diff} curve in eqn. (6) with ΔH_{vH} being an adjustable parameter. Figure 17 shows again the experimental curves of the DMPC/DMPE mixtures of Fig. 16 together with the curves calculated from the phase diagram according to the lever rule [57]

$$C_{\text{diff}}(T) = \frac{x_1^{\text{lc}}\,\Delta H_1 + x_2^{\text{lc}}\,\Delta H_2}{x_2^{\text{g}} - x_2^{\text{lc}}}\Theta^{\text{g}}\frac{\mathrm{d}x_2^{\text{g}}}{\mathrm{d}T} + \frac{x_1^{\text{g}}\,\Delta H_1 + x_2^{\text{g}}\,\Delta H_2}{x_2^{\text{g}} - x_2^{\text{lc}}}\Theta^{\text{lc}}\frac{\mathrm{d}x_2^{\text{lc}}}{\mathrm{d}T} \qquad (16)$$

and then convoluted with a function similar to eqn. (6). The parameters obtained from the simulations are shown in Table 2. The simulations show that ΔH_{vH} decreases in mixtures going through a minimum. This behaviour has been predicted by Sugar [55]. This decrease in cooperativity causes the deviations of the corrected points in the phase diagram of Fig. 16 from the calculated liquidus and solidus lines using the parameters in Table 2. This shows that the decrease in cooperativity has to be taken into account when binary mixtures are analyzed applying thermodynamic theories. Without these corrections the non-ideality parameters obtained from the analysis of the phase diagram are usually higher.

Numerous other lipid mixtures have been investigated and analyzed including those that show peritectic behaviour such as the DMPC/DSPE

TABLE 2

Simulation parameters for DSC curves of DMPC/DMPE mixtures using the model described in the test [23,119]

	a (cal mol^{-1})	b (cal mol^{-1} K^{-1})	A_{298} (cal mol^{-1})	ΔG^{E}_{298} (cal mol^{-1})	$\overline{\Delta H}^{E}_{298}$ (cal mol^{-1})	$\overline{\Delta S}^{E}_{298}$ (cal mol^{-1} K^{-1})
Gel phase	4430	14	258	65	1107	3.5
L.c. phase	500	1	202	50	125	0.25

	Mole fraction, x_{DMPE}					
	0.0	0.1	0.25	0.5	0.75	1.0
ΔH_{vH} (kcal mol^{-1})	1700	450	300	350	400	1260

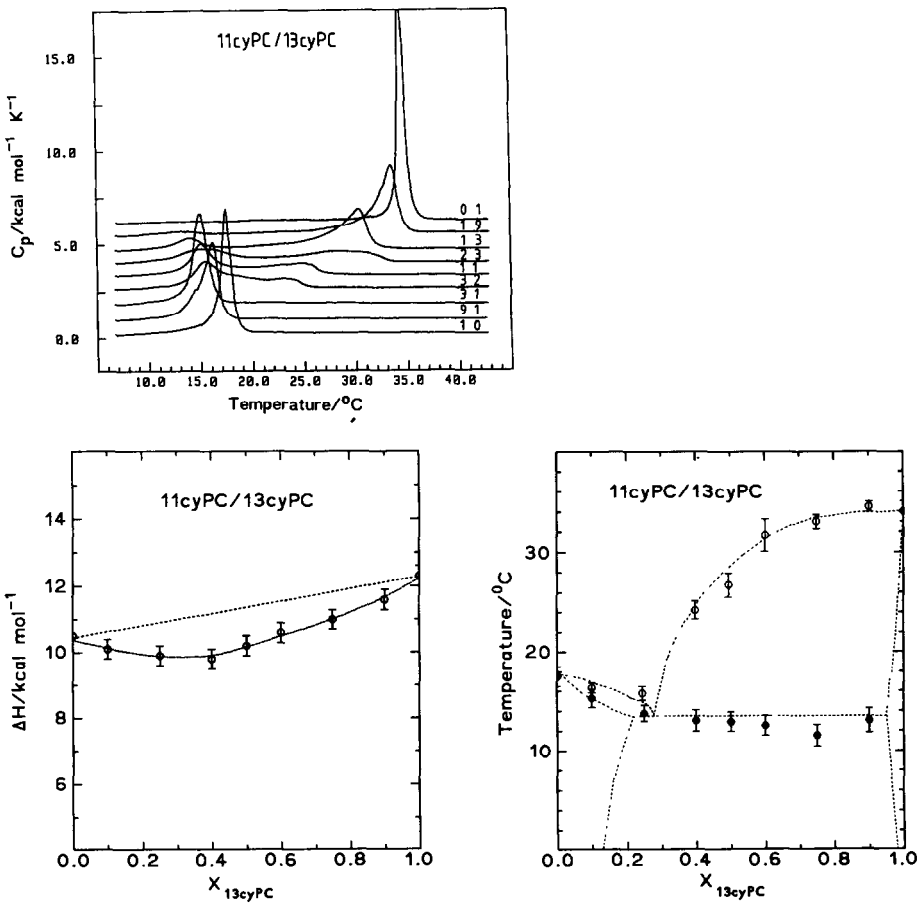

Fig. 18. Top: DSC scans of 11cyPC/13cyPC mixtures at various ratios as indicated. Bottom: (left) dependence of ΔH_{cal} on composition and (right) phase diagram obtained after correction for the finite width of the transition of the pure component (from ref. 58).

system of Fig. 15, or those that display eutectic behaviour. An example for the latter type of mixtures is shown in Fig. 18 where the phase diagram for 1,2-di-(ω-cyclohexyl)undecanoyl-phosphatidylcholine (11cyPC) with 1,2-di-(ω-cyclohexyl)tridecanoylphosphatidylcholine (13cyPC) is displayed [41,58]. These lipids with cyclohexyl groups at the end of saturated chains occur in the thermoacidophilic *Bacillus acidocaldarius* [59,60]. Despite identical head groups and a chain length difference of only two CH_2 groups the system displays a miscibility gap in the gel phase and eutectic behaviour. This indicates that for the packing of these chains large constraints exist due to the bulky terminal cyclohexyl groups. Formation of eutectic mixtures seems to be characteristic for these lipids as similar binary phase diagrams were determined for 11cyPC/14cyPC, 13cyPC/DMPC, 13cyPC/DPPC, and 13cyPC/17isoPC [58]. Eutectic behaviour has also been postulated and found for mixtures of lipids with mixed saturated chains [50,51,54,61].

Influence of pH and ion binding on lipid phase behaviour

The state of ionization of the head group has a strong influence on the thermotropic properties of phospholipids. PCs and PEs remain zwitterionic over a large pH range, the phosphate group becoming protonated only at very low pH. For PEs the pK of the ammonium group is very high, the dissociation occurring at pH values larger than 11.5 [1]. For phospholipids which are negatively charged at pH 7 such as phosphatidic acids (PA), phosphatidylglycerols (PG), or phosphatidylserines (PS), this is different, as the transition properties depend more strongly on pH and ionic strength of the solution. The degree of ionization of phospholipids as a function of pH is schematically shown in Fig. 19 [1]. For PAs the transition temperature increases when the pH is lowered toward 4.5. Further protonation leads to a dehydration of the bilayers and the dispersion is no longer stable. The

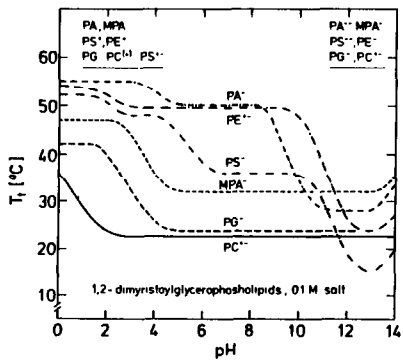

Fig. 19. Schematic drawing of the dependence of the transition temperature T_t for dimyristoyl phospholipids on pH (from ref. 1).

TABLE 3

Transition temperatures and transition enthalpies for some phospholipids as a function of pH

Lipid	n	pH	T_m (°C)	ΔH_{cal} (kcal mol^{-1})	Ref.
PA	14:0 [c]	3.5	55.0	3.7	63
	[c]	6.0	52.2	5.7	63,109
	[c]	12.0	22.4	4.1	63
	15:0 [a]	6.0	40.0	3.5	65
	[a]	12.2	19.0	2.5	65
	16:0 [c]	6.0	65.0	7.9	23,109
	[c]	12.0	43.1	5.7	23,109
	[b,c]	3.5	75.0	2.8	63
	[b,c]	6.0	73.3	7.1	63
	[b,c]	12.0	53.8	5.8	63
PG	16:0 [c]	8.0	43.5	10.0	119
	[c]	2.7	59.0	9.2	119

[a] 1,2-Dipentadecylmethylidene phosphatidic acid [65].
[b] Ether lipid 1,2-dihexadecyl phosphatidic acid [63].
[c] In water without added salt, $c \approx 2$–3 mM.

transition temperature decreases again slightly [62,63]. At high pH the dissociation of the second proton of PA has an apparent pK of about 10 at low ionic strength. The transition temperature decreases drastically. This decrease is due to electrostatic effects, changes in tilt angle of the chains and changes in hydration [1,62–66]. Table 3 shows some calorimetric data for PAs and DPPG as a function of pH.

Binding of divalent cations to zwitterionic phospholipids such as DPPC or DPPE does not lead to drastic changes of the thermotropic behaviour as long as the ion concentration stays low [66]. This is different for trivalent cations such as Fe^{3+} or La^{3+} which have much higher binding constants to PC [24,66,67]. Addition of La^{3+} to DPPC reduces the ΔH value of the pre-transition, the main transition being at first unaffected. La^{3+} causes a change of the tilt angle of the acyl chains from 30° ($L_{\beta'}$ phase) to 0° (L_{β} phase). Another special case where large changes in thermotropic behaviour are observed is the binding of UO_2^{2+} ions to DPPC [68]. Uranyl ions at molar ratios of 1/10 decrease the tilt angle of the DPPC chains. Further addition of UO_2^{2+} leads to a drastic increase in transition temperature, the binding inhibiting the rotational motion of the molecules in the gel phase [68]. Figure 20 shows DSC scans of DPPC/UO_2^{2+} at various molar ratios together with the dependence of the transition enthalpy which is continuously decreasing upon UO_2^{2+} addition [68].

Binding of univalent cations to negatively charged lipids such as PA, PG, or PS is usually weak with the exception of Li^+ ions [1,24]. However, the transition temperature shows a dependence upon the ionic strength of the

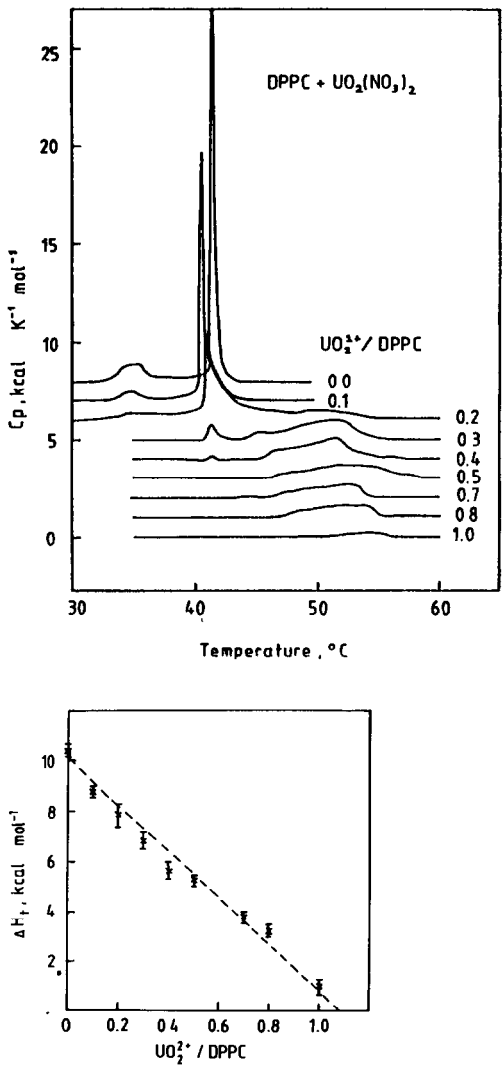

Fig. 20. Top: DSC curves of DPPC with increasing amounts of uranylacetate. Bottom: dependence of ΔH_{cal} on the UO_2^{2+} /DPPC ratio (from ref. 68).

solution. Usually an increase in T_m is found with increasing concentration, the slopes depending on the size of the cation, an exception being large cations such as the tetramethyl-ammonium ion. The shift can be analyzed using the Gouy–Chapman theory of the electrical double layer and including hydration effects [1,24]. PGs when dispersed in pure water swell indefinitely. The transitions of the resulting aggregates are very broad and ill-defined. Addition of 100 mM NaCl or KCl leads to well defined main transitions at reduced temperature. This effect is more pronounced for the shorter chain homologues. In Fig. 21 the behaviour of DPPG at low

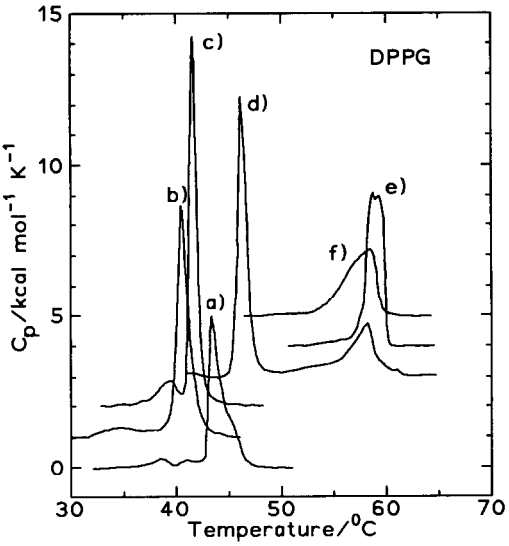

Fig. 21. DSC scans of DPPG under various experimental conditions: (a) in pure water, (b) 100 mM NaCl, (c) 1 NaCl, (d) 3 M NaCl, (e) at pH 2.7, (f) with $CaCl_2$ at a ratio of 1:1. DPPG concentration was 2.5 mM [119].

concentration (1 mM) is shown under various conditions. The effect of the dependence of ΔH_{cal} and T_m on the ionic strength of monovalent salts has to be taken into account when calorimetric data obtained by different groups using different instruments are compared. For instance, DSC curves of PGs from DSC instruments of the heat conduction type are usually obtained at much higher lipid concentrations so that the ionic strength is also much higher. In addition the higher heating and cooling rates used with these instruments can sometimes lead to metastable phases which are not observed when adiabatic DSC instruments are used [69].

Divalent and trivalent cations bind much more strongly to negatively charged lipids and numerous DSC studies have been performed (see refs. 1 and 24 for reviews). Binding of divalent cations to negatively charged lipids also depends on the total lipid concentration and on the concentration of monovalent salts. Thus binding constants obtained for binding of divalent cations vary greatly with experimental conditions. Figure 21 shows that binding of Ca^{2+} to DPPG at low ionic strength (about 2.5 mM) at a molar ratio of 1:1 shifts the transition temperature to about 58 °C, a value only slightly lower than T_m of DPPG at pH 2.7 [23,118]. This shows that Ca^{2+} as well as H^+ is effective in neutralizing the charge and can lead to similar hydration states of the PG head group. At higher Ca^{2+} concentration and higher ionic strengths Ca^{2+} shifts the T_m to about 90 °C and, depending on the scan rate, multiple peaks are observed [69].

For DMPA at 1–2 mM concentration the binding of Ca^{2+} shifts the transition temperature from 52 to 61 °C. In binary mixtures with DMPC

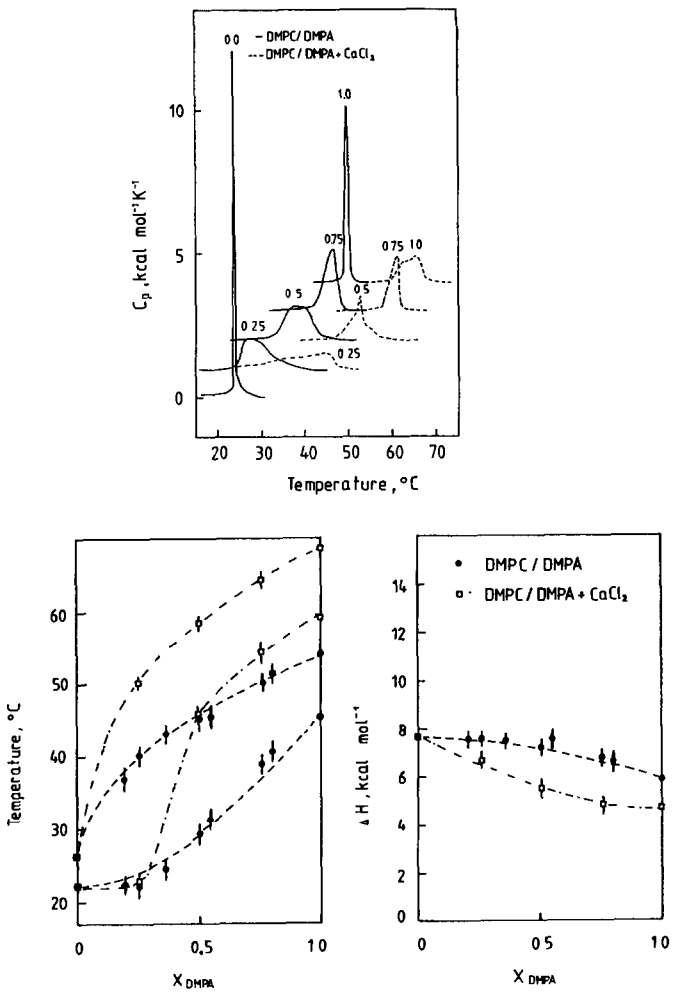

Fig. 22. Top: DSC scans of DMPC/DMPA mixtures without and with Ca^{2+} at a ratio of 1:1. Bottom: (left) Uncorrected phase diagram for DMPC/DMPA with (□) and without (●) Ca^{2+} (1:1) and (right) dependence of ΔH_{cal} on composition (from refs. 23, 119).

the binding of Ca^{2+} changes the miscibility from an almost ideal mixing behaviour to a system with an indication for a miscibility gap in the gel phase as shown in Fig. 22. Similar behaviour is found for the system DPPC/DMPA [23,118]. These mixed systems are interesting from a biological point of view as in the liquid-crystalline phase Ca^{2+} binding can lead to cluster formation as shown by spectroscopic techniques [70,71].

Lipid–cholesterol mixtures

Because cholesterol is present in membranes of most eukaryotic cells in high amounts (up to 50 mol%) lipid–cholesterol mixtures have been

studied in some detail (for reviews see refs. 72 and 73). It was first shown by Ladbrooke et al. [7] that addition of cholesterol to DPPC causes a disappearance of the pre-transition at about 5 mol% cholesterol, the main transition broadening at higher concentrations and finally disappearing at 50 mol% cholesterol. These original findings were later verified using DSC instruments with higher sensitivity [74–76]. It was shown that at cholesterol concentrations below 20 mol% the calorimetric endotherm could be decomposed into a broad and a narrow peak, the broad peak remaining at cholesterol concentrations above 20 mol% and gradually decreasing in area. Numerous attempts have been made to describe the behaviour of DPPC/cholesterol mixtures in terms of a phase diagram and phase boundaries below T_m between 20 and 25 mol% cholesterol have been suggested using the results obtained by various other physicochemical techniques [76–79]. On the basis of NMR spectroscopy it was shown that exchange between different lipid species, presumably belonging to different phases, is relatively fast, so that the domains of different composition cannot be very large [80,81]. Theoretical phase diagrams have been calculated on the basis of a microscopic interaction model [82,83]. These calculations showed that cholesterol can accumulate at domain boundaries, the domains being of a size of approximately 10–40 molecules [83]. Despite all efforts the exact shape of the phase diagram and the microscopic structure of lipid–cholesterol lamellar phases are still not completely understood. It is clear that cholesterol, due to its rigid ring system, acts as a spacer between the acyl chains separating the lipid molecules so that they gain more freedom

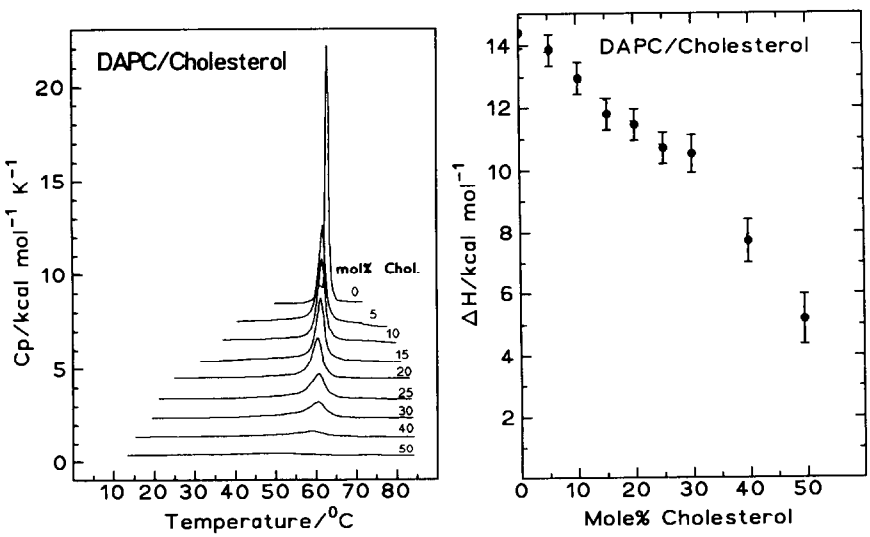

Fig. 23. Left: DSC scans of DAPC/cholesterol mixtures with increasing cholesterol concentration. Right: dependence of ΔH_{cal} on cholesterol content [119].

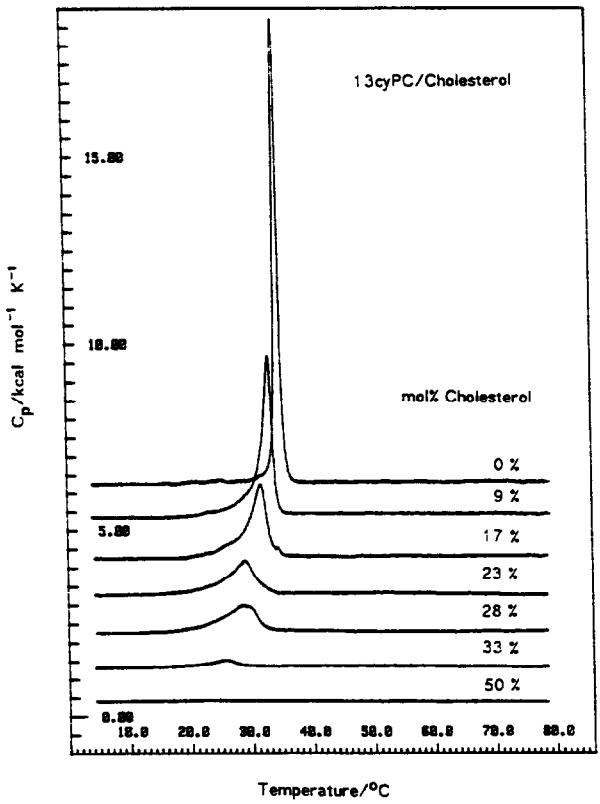

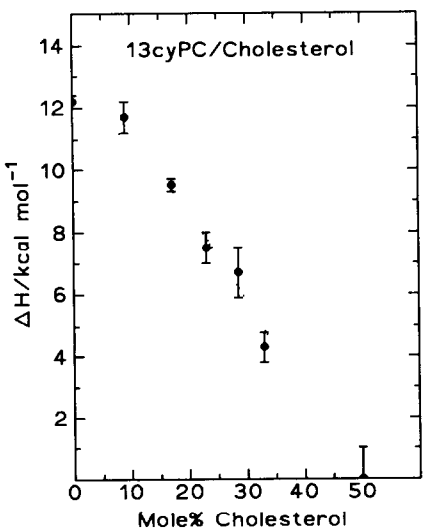

Fig. 24. Top: DSC scans of 13cyPC/cholesterol mixtures with increasing cholesterol concentration. Bottom: dependence of ΔH_{cal} on cholesterol content (from ref. 58).

for rotation. The acyl chains are transferred into an intermediate state between gel and l.c. state. Relative to the l.c. phase trans–gauche isomerization is reduced (this is the so called condensation effect of cholesterol), but relative to the gel phase trans–gauche isomerization is slightly higher and rotational mobility is greatly increased.

For a particular phospholipid class the effect of cholesterol depends on the chain length. Whereas the broad transition in DMPC/cholesterol and DPPC/cholesterol mixtures appears at higher temperatures relative to the sharp peak of the main transition [74–76], this is reversed in longer chain PCs such as DAPC [119]. This is shown in Fig. 23. Even at 50 mol% cholesterol a very broad transition is still present with a transition enthalpy of about 4 kcal mol^{-1} (only discernible in Fig. 23 after ordinate expansion). These findings are at variance with recent reports by Singer and Finegold [84,85] who reported a systematic study of the effects of chains length of PCs on the mixing behaviour with cholesterol. These authors reported a disappearance of the phase transition of DAPC at 43.3 or 49.5 mol% cholesterol, respectively [84,85].

The effect of cholesterol is qualitatively similar when incorporated into bilayers of other lipid classes as long as the fatty acyl chains are saturated (see refs. 15, 16, 23, 24, 73, 73, 80, 81, 86, 87 for details). When unsaturated, branched-chain or, for instance, ω-cyclohexyl fatty acids are esterified to the lipid, cholesterol has varying effects, probably due to different solubilities in the lamellar phases and different packing requirements in the gel phase. Thus it appears as if phase separation due to limited miscibility in the gel phase can occur. An example for this effect is shown in Fig. 24 for the system 13cyPC/cholesterol [58,119]. In this mixture the sharp peak corresponding to the main transition of the pure lipid is still visible at 33 mol% cholesterol.

Lipid–protein interactions

Biological membranes are composed of lipids and proteins. The lipids provide the basic permeability barrier, the bimolecular lipid membrane. Membrane proteins are either incorporated into the bilayer — they can even span the bilayer — or they are bound to the surface of the membrane by electrostatic forces. The fluid-mosaic model of the membrane proposed by Singer and Nicolson [88] is the widely accepted model for the general structure of a biological membrane. As the bilayer is the basic structure of a biological membrane, phase transitions in natural membranes should be detectable by DSC. This is indeed the case and was one of the proofs that lipids in membranes are really arranged in a bilayer. It was first shown by the pioneering DSC work of Steim et al. [89]. A more recent example is shown in Fig. 25 where DSC scans of the cell envelope, the outer membrane and the extracted lipopolysaccharide of *Salmonella minnesota* (mutant

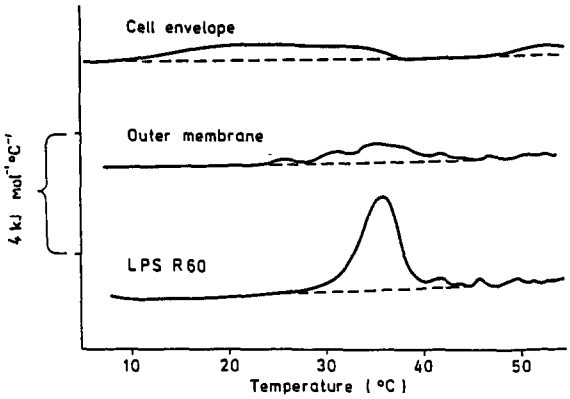

Fig. 25. DSC scans of the cell envelope, the outer membranes and the extracted lipopolysaccharides of *Salmonella minnesota* mutant strain R 60 (from ref. 90).

strain R 60) are shown [90]. Phase transitions in natural membranes are very broad because the lipids are a complex mixture and the proteins lower the cooperativity of the phase transition even further. The DSC scans are therefore difficult to analyze. For these reasons lipid–protein interactions have been studied in much detail during the last few years using reconstituted model systems. Several reviews have appeared about lipid–protein interactions [15,20,91]. DSC studies can provide information on the type of interactions between proteins and lipids by recording the transition peaks as a function of protein content in the lipid bilayer. Papahadjopoulos [91] suggested three types of basic interactions that can be expected and which lead to characteristic changes in the DSC peaks.

(1) Electrostatic interactions often lead to an increase in ΔH_{cal} with a concomitant increase in transition temperature.

(2) Electrostatic surface binding followed by partial penetration into the bilayer leads to more drastic changes of ΔH_{cal} and T_m, the values usually being decreased because the chain interactions are reduced.

(3) Pure hydrophobic interactions of integral membrane proteins lead to a linear decrease of ΔH_{cal} with protein content, a broadening of the transition and only slight changes in T_m. In this case the number of lipid molecules in the lipid annulus surrounding the protein, the "solvation shell", can be determined from the slope of ΔH_{cal} versus protein/lipid ratio.

In reality the situation is more complex as combinations of these three basic types of behaviour can be found. In addition several overlapping DSC peaks are sometimes observed. To give a few examples, lipid–protein interactions in model systems have been studied using synthetic polypeptides [92,93], glucagon [94], proteolipid apoprotein of bovine myelin [95], human myelin basic protein [96], bacteriorhodopsin [97,98], cytochrome oxidase [99,100], apolipoprotein A-II [101], cytochrome *c* [102], (Ca^{2+}–

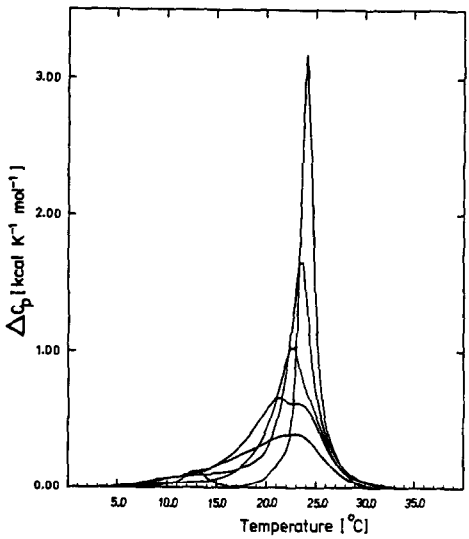

Fig. 26. DSC scans of DMPC vesicles with increasing mounts of bacteriorhodopsin with the following lipid/protein ratios: ∞, 552, 316, 188, and 91 (from ref. 97).

Mg^{2+})-ATPase [103], melittin [24,104,105] and numerous other peptides and proteins (see refs. 15, 16, 20). Only two examples will be shown to illustrate the effects of peptides and proteins on the phase transition behaviour of lipids.

The first example is the hydrophobic membrane spanning protein bacteriorhodopsin (BR), which was reconstituted into DMPC bilayers at several different lipid/protein ratios [97]. Figure 26 shows the DSC peaks observed with this system as a function of protein content. BR should belong to the third class of proteins mentioned above as it spans the lipid bilayer and is very hydrophobic. However, not only a broadening of the phase transition with a decrease of transition enthalpy is observed but also a shift of T_m to lower temperature. At low temperature in the gel phase BR aggregates in lipid membranes into a hexagonal lattice. Taking this process into account the number of lipid molecules in the first "solvation shell" can be calculated as 60, a value which is somewhat higher than the value obtained from the slope of a plot of ΔH_{cal} versus the protein/lipid ratio [97,98].

The second example is the amphiphilic polypeptide melittin, which has 26 amino acids and forms a bent α-helix [106]. In aqueous solution the polypeptide aggregates into tetramers due to its amphiphilic nature. In the presence of lipid bilayers melittin partitions into the membrane and finally disrupts the bilayers [104,105,107]. In DSC experiments of DMPC/melittin vesicle systems a decrease of the transition enthalpy with only slight changes in T_m were observed [23,104,105]. The decrease of ΔH_{cal} is not linear, probably due to changes of the state of aggregation of melittin in

the bilayer. For other phospholipid membranes the changes in transition behaviour depend on the charge of the lipid head group and on the head group interactions. For DMPA a slight shift of T_m to higher temperature

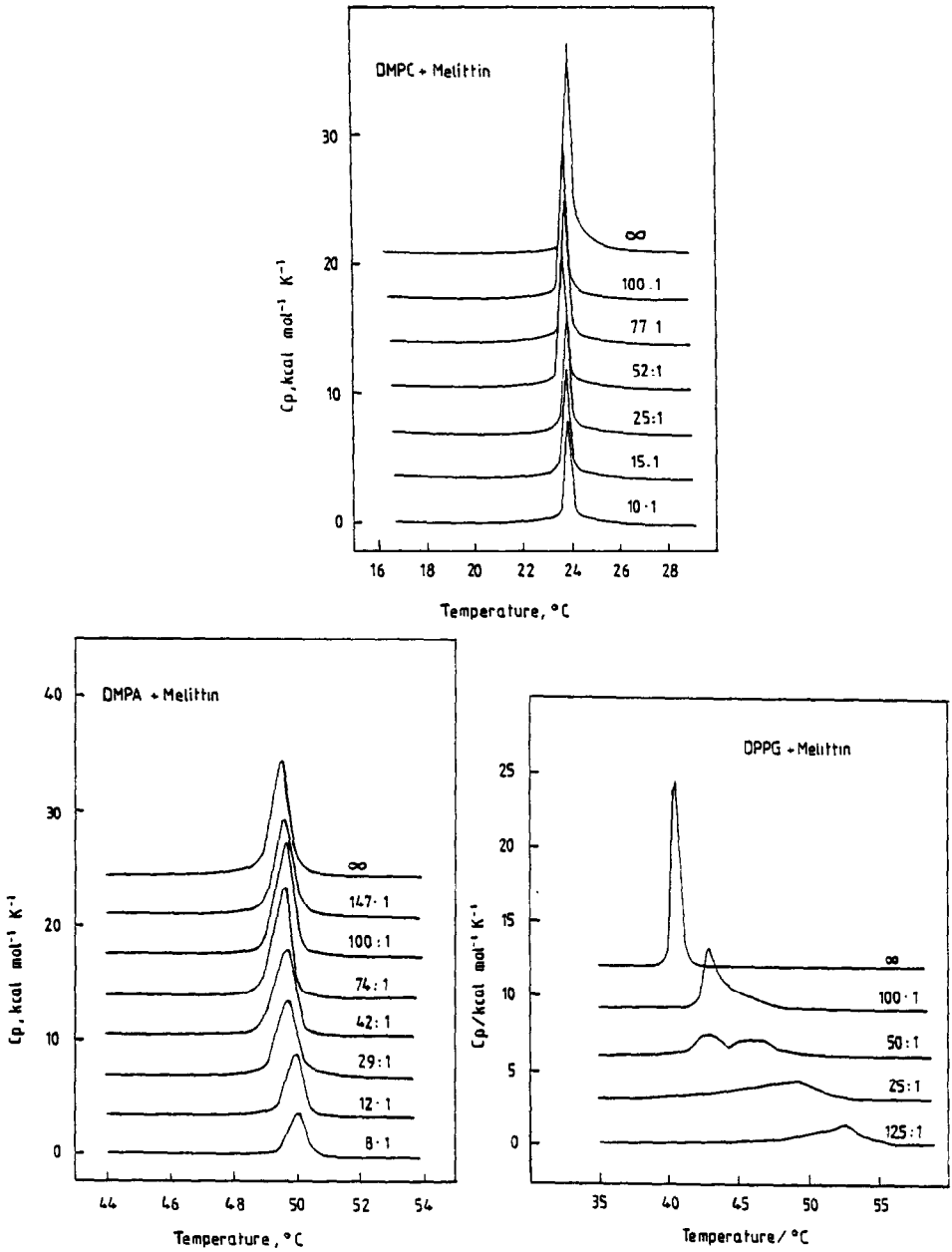

Fig. 27. DSC scans of DMPC, DMPA, and DPPG with increasing amounts of melittin at the indicated lipid/peptide ratios (from ref. 23).

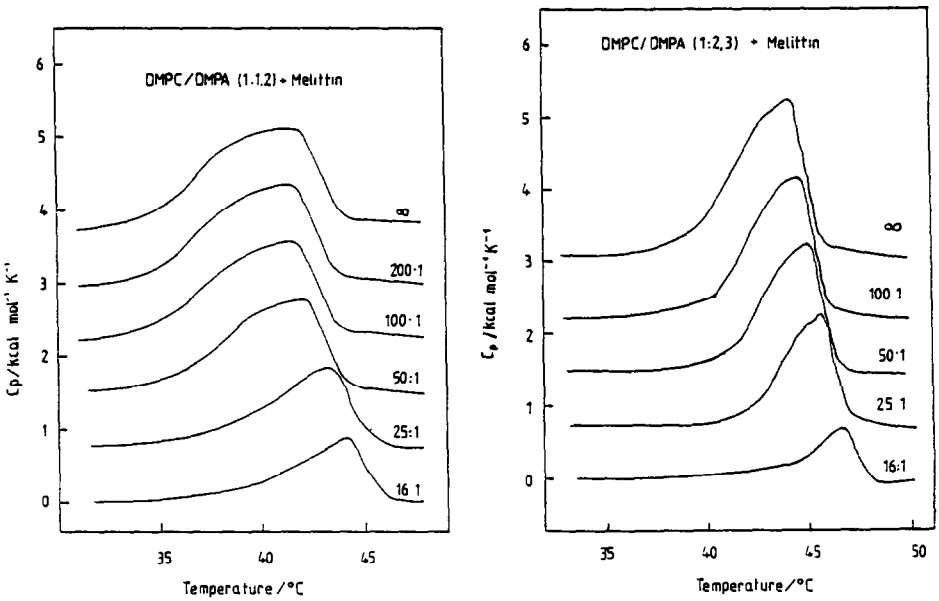

Fig. 28. DSC scans of two different DMPC/DMPA mixtures with increasing amounts of melittin as indicated (from refs. 23, 119).

was observed whereas for PGs a large increase of T_m with a broadening of the phase transition can be seen. These three different types of interaction of melittin with phospholipids are shown in Fig. 27 [23,119]. The shifts of T_m observed for DPPG are due to electrostatic interactions, as melittin has four positive charges at the N-terminus. This terminus extends into the water phase, but is probably located close to the lipid head groups [106]. In DMPA the electrostatic shift is much smaller, because for PA strong intermolecular hydrogen bonds between the phosphate head groups lead to higher T_m values overcompensating the repulsive electrostatic effects, which would lead to a lower T_m. In DMPC/DMPA mixtures the hydrogen bonds are broken, because this mixture shows almost ideal mixing behaviour. The electrostatic effect caused by melittin is now much larger and T_m is raised much more than in the pure systems DMPA or DMPC as shown in Fig. 28. In all cases plots of ΔH_{cal} versus melittin content are non-linear, as mentioned above, indicating changes in the state of aggregation of melittin and also of the lipids. At high melittin content small disc-like aggregates have been observed by electron microscopy [107].

Apparent molar heat capacities of lipids

DSC has also been used to determine the apparent molar heat capacities of phospholipids [108–110]. With a sensitive DSC instrument of the adiabatic type, which has sufficient baseline stability and reproducibility the

TABLE 4

Apparent molar heat capacities ${}^{\Phi}C_p$ (cal mol^{-1} K^{-1}) at temperatures $\Delta T = T - T_m$ in the gel and l.c. phase (from ref. 109)

Lipid	n	pH	ΔT (°C)	
			−20	+10
PC	14:0		270	305
	16:0		380	410
	18:0		470	450
	20:0		580	480
PE	12:0		260	305
	14:0		350	355
	16:0		430	400
	18:0		480	400
	20:0		560	445
PA	14:0	6	380	250
		12	295	380
	16:0	6	426	290
		12	412	420

apparent molar heat capacity ${}^{\Phi}C_p$ can be calculated from the shift of the base line Δ when the sample is in the cell compared with a solvent filled cell according to [111]

$$ {}^{\Phi}C_p = \left[c_{pw}(v_1/v_w) - \Delta/m_1\right]M_1 \tag{17} $$

where c_{pw} is the specific heat of water, v_1 and v_w are the specific volumes

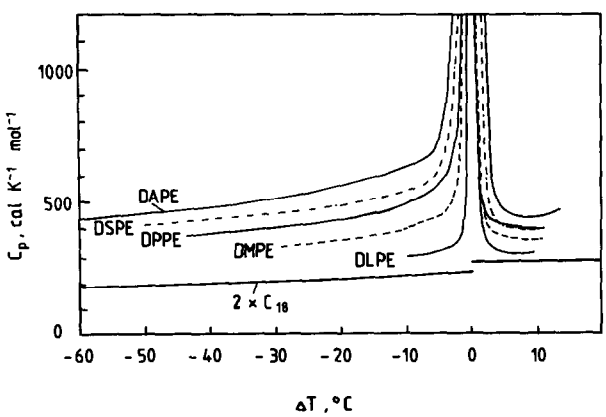

Fig. 29. Apparent molar heat capacities of different PEs as a function of reduced temperature $\Delta T = T - T_m$. The transition peaks are off-scale. Included is the temperature dependence of two C_{18} chains in the solid and liquid state to illustrate the difference in heat capacity (from ref. 109).

of lipid and water, respectively, and m_1 and M_1 are the mass and molecular weight of the lipid. Table 4 shows values of the apparent molar heat capacities of several lipids above and below the phase transition temperature and Fig. 29 shows DSC scans of PEs with different chain lengths on a reduced temperature scale [109]. Included in this figure is a calculated curve for two C_{18} alkane chains in the solid and liquid state to illustrate the differences in heat capacity. The experimental ${}^{\Phi}C_p$ values are considerably larger than heat capacity values calculated from group contributions of the acyl chains, the glycerol backbone and the hydrated head group. This indicates that "hydrophobic hydration", i.e. contributions from changes in the structure of water which is in contact with hydrophobic groups, has to be taken into account. Similar effects have also been observed for proteins, though protein denaturation is accompanied by a considerable change in heat capacity, which does not occur during the lipid phase transition [110].

REACTION CALORIMETRY

Instrumentation

In membrane studies reaction calorimetry can be used to measure heats of ion binding to lipid bilayers and heats of incorporation of various molecules including peptides into lipid membranes. Also ion induced phase transitions at constant temperature can be investigated. Only a few studies of this type have been performed up to now [23,94,101], but the application of reaction calorimetry to membrane systems will certainly increase in the future. In all previous studies mainly two reaction calorimeters, which are sensitive enough for this type of work, have been used. The first one is the LKB-Batch-Calorimeter Model 10700, which has later been upgraded by a titration accessory [112] and the OMEGA titration calorimeter (Microcal Inc., Amherst, MA, USA) developed on the basis of the Microcal MC 2 DSC instrument [113].

Heats of ion binding

Phospholipids such as PAs and PGs show pH dependent ionization and transition behaviour (see above). For instance, DMPA can be titrated with OH^- according to

$$DMPA^- + OH^- \rightleftharpoons DMPA^{2-} + H_2O \qquad (18)$$

The observed reaction enthalpy ΔH_R will be the sum of the dissociation enthalpy ΔH_{Diss} of DMPA and the neutralization enthalpy of water ΔH_{Neutr}. In a batch type experiment the total dissociation enthalpy is determined by addition of OH^- to totally dissociate the second proton. For DMPA a pH jump to pH 12 is sufficient. We have measured the tempera-

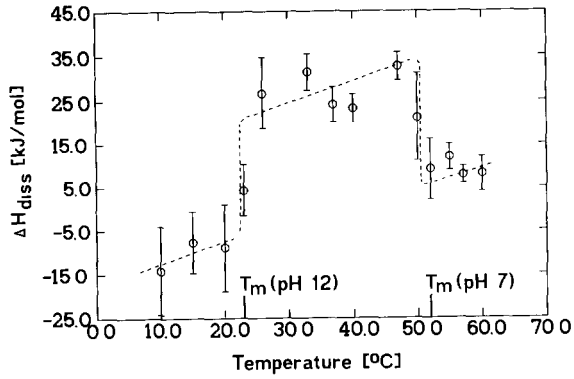

Fig. 30. Temperature dependence of the enthalpy of dissociation ΔH_{Diss} for the reaction $DMPA^- + OH^- \rightleftharpoons DMPA^{2-} + H_2O$ determined by batch calorimetry. The heat of neutralization of water has already been subtracted. Transition temperatures of DMPA at pH 7 and 12 are indicated. At these temperatures jumps occur due to pH induced phase transitions [120].

ture dependence of the dissociation enthalpy of $DMPA^-$ over a wide temperature range, covering the phase transitions to the l.c. phase of both $DMPA^-$ and $DMPA^{2-}$. The results are shown in Fig. 30 [23,120]. At temperatures below T_m ΔH_{Diss} includes the ΔH contribution from a change in tilt angle of the hydrocarbon chains as the gel phase changes from an L_β to an $L_{\beta'}$ phase [64]. Between the transition temperature of the doubly charged form of DMPA at 23 °C and the singly charged form at 51 °C ΔH_{Diss} is the sum of the heat of dissociation and the heat of transition as deprotonation induces a phase transition from the gel phase to the l.c. phase. Above 51 °C the bilayer is in the l.c. state and the heat of reaction is the true ΔH_{Diss} value for dissociation in the l.c. state. The jumps in ΔH_{Diss} correspond well with the transition enthalpies of $DMPA^{2-}$ at $T_m = 23$ °C and $DMPA^-$ at 51 °C.

In all three temperature ranges ΔH_{Diss} shows a positive temperature dependence, which means that there is a positive ΔC_p between singly and doubly charged DMPA. This agrees with values for the apparent molar heat capacities measured for $DMPA^-$ and $DMPA^{2-}$ by DSC, where doubly charged PAs had higher ${}^{\Phi}C_p$ values than the singly charged form [109]. The higher apparent molar heat capacity for $DMPA^{2-}$ can be explained by an increase in "hydrophobic hydration" for the doubly charged form, as the packing of the hydrocarbon chains is changed by an increase in tilt angle caused by the larger electrostatic repulsion of the head groups and increased hydration.

The dissociation reaction can also be followed by using titration calorimetry. Figure 31 shows an experimental titration curve of $DMPA^-$ with NaOH at 75 °C and the integral heat of reaction as a function of added NaOH. The residual small peaks in the experimental curve are due

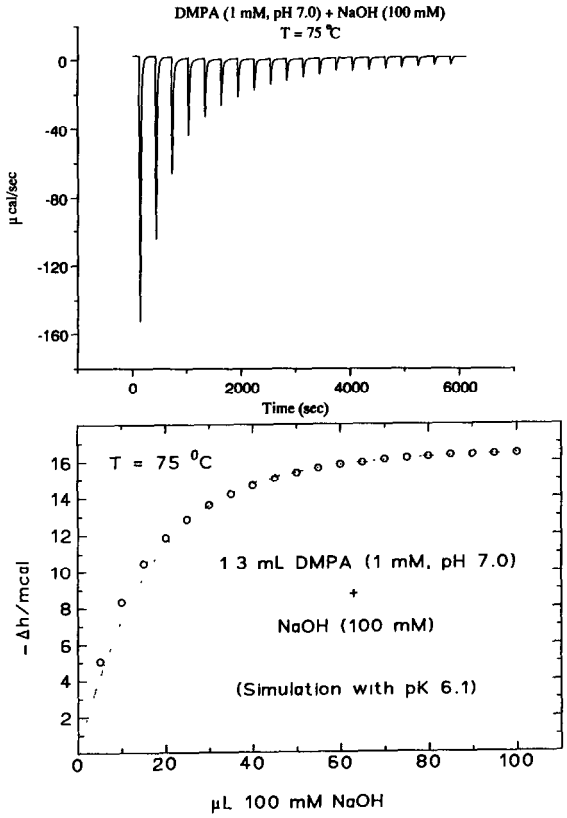

Fig. 31. Top: experimental calorimetric titration curve of DMPA at high temperature in the liquid-crystalline phase. Similar titration curves can be obtained at lower temperatures. Bottom: integral heat of reaction as a function of added NaOH. The dashed curve is calculated using an intrinsic pK_0 of 6.1 [120].

to the heat of dilution of NaOH to the DMPA dispersion and have been subtracted in the lower curve [23,120]. The titration curve can be calculated by using the Gouy–Chapman theory with the intrinsic pK_0 as an adjustable parameter [1,23,24,114,115]. A good fit of the experimental curves was obtained with a value of 6.1 for the intrinsic pK_0 taking into account the changing ionic strength of the dispersion in the course of the titration, as the sample had no additional salt. The apparent pK_0 of DMPA taking into account only the electrostatic effects is defined by [114]

$$pK_{app} = pK_0 + (e\psi_0/2.303kT) \tag{19}$$

with ψ_0 being the surface potential and e the electric charge. The value of pK_{app} is much higher under the experimental conditions, namely approximately 10 [1,24,62,63]. The intrinsic pK_0 for DMPA determined from the simulations is close to the pK of the water soluble compound glycero-3-phosphate which represents the head group of DMPA and for which no

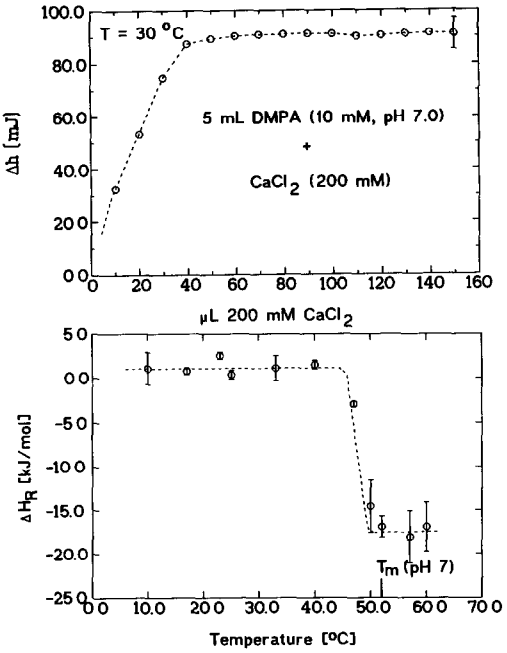

Fig. 32. Top: integral heat of reaction for the binding of Ca^{2+} to $DMPA^-$ as a function of added Ca^{2+}. The error bar at the last point indicates the value for the binding enthalpy determined in a batch experiment. Bottom: dependence of the heat of reaction for Ca^{2+} binding to $DMPA^-$ as determined in a batch experiment [121].

electrostatic surface effects are expected. The pK of glycero-3-phosphate is 6.65 at 20 °C and shows only a small temperature dependence. These results show that the Gouy–Chapman theory is sufficient to describe the dissociation behaviour of PAs. The intrinsic pK_0 of DMPA calculated at other temperatures is similar, which shows that also for DMPA the temperature dependence of the intrinsic pK_0 is negligible in contrast to the apparent pK which strongly depends on the surface charge density and is thus lower for lipids in the liquid-crystalline phase [114,115].

As an example for the binding of divalent cations a titration of $DMPA^-$ with Ca^{2+} is shown in Fig. 32 [23,121]. At 30 °C in the gel state of DMPA the heat of Ca^{2+} binding is positive. The titration curve can in principle be simulated using the Gouy–Chapman theory assuming 1 : 2 binding for Ca^{2+} to $DMPA^-$. The general shape of the titration curve can be well reproduced by these calculations but because of the high binding constant of Ca^{2+} the experimental points are not precise enough at the moment to exactly determine the intrinsic binding constant, which is estimated from the titration experiment to be around 10 M^{-1}. The apparent binding constant is of course much higher. Because of the imprecision of the data it can not be excluded that the simple model of 1 : 2 binding is wrong and that

1:1 binding can also occur. The temperature dependence of the heat of Ca^{2+} binding to $DMPA^-$ as determined by a batch experiment is shown in Fig. 32 at the bottom. Below T_m the temperature dependence of the heat of Ca^{2+} binding is almost negligible. At T_m a large jump in ΔH_R occurs as now a transition from the l.c. phase to a gel phase with bound Ca^{2+} is induced. The differences between ΔH_R values measured below and above T_m correspond roughly to the transition enthalpy of $DMPA^-$ as measured by DSC.

Heats of incorporation of peptides

Titration calorimetry can also be used to study the interaction of proteins and peptides with lipid bilayers. Experiments of this type have been performed for instance with glucagon [94] and apolipoprotein A-II [101]. It was found that the heat of incorporation of these amphiphilic proteins into bilayers changes sign at the transition midpoint, being positive below and negative above T_m. Figure 33 shows titration experiments with the polypeptide melittin, DSC experiments for which have been described above [23]. The heat of incorporation of melittin into DMPA bilayers is negative above T_m and positive below T_m as reported for other proteins mentioned above. The positive reaction enthalpy below T_m is caused by the disruption of the lipid packing due to the perturbation of the chains by the incorporated peptide. Above T_m the chains in the lipid annulus around the peptide are somewhat ordered with respect to the free lipid in the l.c. state, the incorporation enthalpy thus becoming exothermic. These effects were also theoretically predicted by Jähnig [116]. Similar effects as for the DMPA system are observed for DMPC.

In the case of PGs the transition temperature is shifted to higher values upon melittin incorporation due to electrostatic effects (see Fig. 26). Below T_m the reaction enthalpy is endothermic throughout, but above T_m the reaction enthalpy changes sign at a certain lipid/melittin ratio due to the shift of the transition temperature upon melittin incorporation. This effect is shown in Fig. 34 for the DPPG/melittin system. The ratio at which the reaction enthalpy changes sign agrees well with the DPPG/melittin ratio at which the transition midpoint of the DSC curve is at the temperature of 45 °C where the titration experiment was performed (see Fig. 26).

Below T_m in the gel phase the kinetics of melittin incorporation are so slow that titration experiments can only be performed at temperatures close to T_m. In the liquid-crystalline phase the kinetics are much faster, so that the temperature dependence of the incorporation enthalpy can be measured. The results of experiments with DMPC and DMPA bilayers are shown in Fig. 35. The heat of melittin incorporation decreases with temperature, indicating that the ordering effect of the peptide on the lipids

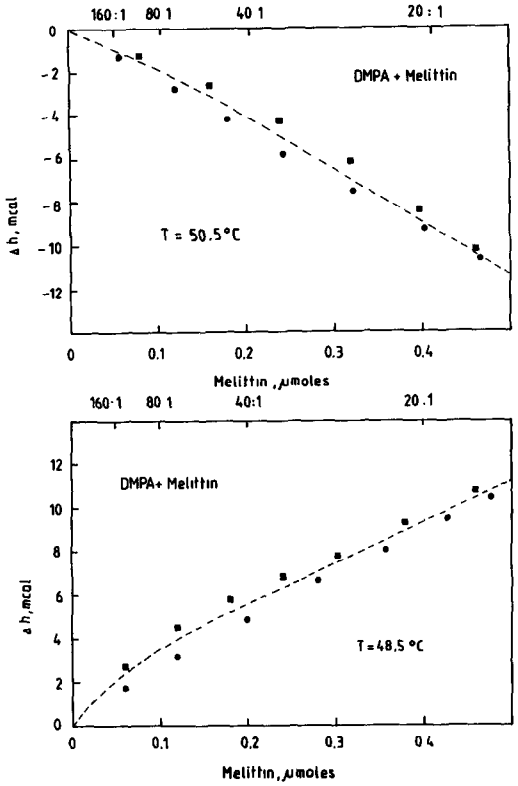

Fig. 33. Top: integral heat of reaction for melittin incorporation into DMPA bilayers in the liquid-crystalline phase. Two different sets of experiments are shown. Bottom: integral heat of reaction for melittin incorporation into gel phase DMPA bilayers. Experimental conditions: 5 ml 1.6 mM DMPA (pH 6) + 4 mM melittin (from ref. 23).

in the annulus is reduced. This effect has also been theoretically predicted by Jähnig [116].

The few examples shown here for the application of reaction calorimetry to membrane systems show that this calorimetric technique is a powerful tool for the analysis of the interactions between lipids and ions or other molecules. Binding constants for ions and other molecules can be determined from simulations of titration curves. From the temperature dependence of these binding constants the van't Hoff enthalpy for the binding reaction can be calculated. As this is the directly measurable quantity in the calorimetric experiment comparisons can be made between calculated and directly measured reaction enthalpies. The calorimetric experiment affords also the temperature dependence of the reaction enthalpy. The ΔC_p values obtained from the slopes of ΔH_R versus temperature provide additional insight into the nature of the binding reaction and into contributions from changes in hydrophilic and hydrophobic hydration.

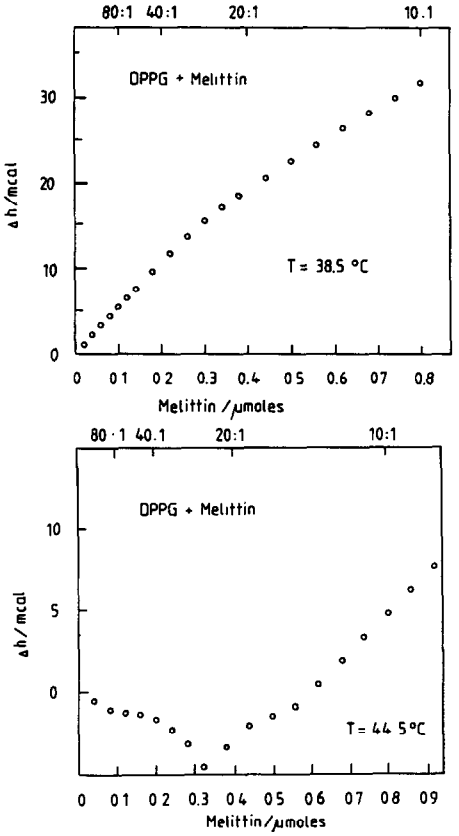

Fig. 34. Top: integral heat of reaction for melittin incorporation into DPPG bilayers in the gel phase at pH 8. Bottom: integral heat of reaction for melittin incorporation into liquid-crystalline DPPG bilayers. The change in sign of the reaction enthalpy is due to the melittin induced shift of T_m. Experimental conditions: 5 ml 1.6 mM DPPG (pH 8)+4 mM melittin [119].

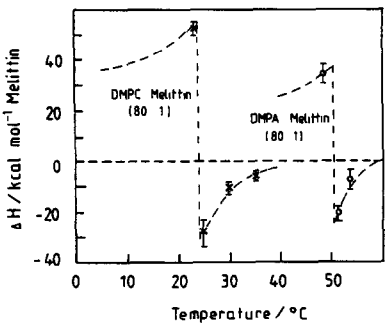

Fig. 35. Temperature dependence of the heat of incorporation of melittin into DMPC and DMPA bilayers at a fixed lipid/peptide ratio (from ref. 23).

CONCLUSIONS

Differential scanning calorimetry has become a standard technique for the analysis of natural membranes and lipid model membranes. Information on transition enthalpies of pure lipids, on lipid miscibilities in binary lipid mixtures, on the effects of ion binding, the energetics of lipid–protein interactions, and on partitioning of solutes into lipid membranes can easily be obtained with relatively little material and in reasonable time due to the high sensitivity of the present commercial adiabatic DSC instruments. Reaction and titration calorimetry has been used very little up to now for the investigation of membrane systems, but the application of these methods will certainly increase in the near future in the same way as has been the case for the DSC method during the last ten years.

ACKNOWLEDGEMENTS

I thank W. Hübner, K. Habel, and J. Tuchtenhagen of my research group for letting me use results of their recent work. The work reported here was supported by grants from the Deutsche Forschungsgemeinschaft and the Fonds der Chemischen Industrie. I thank these organizations for their financial support.

REFERENCES

1 G. Cevc and D. Marsh, Phospholipid Bilayers: Physical Principles and Models, Wiley, NY, 1987.
2 R.B. Gennis, Biomembranes: Molecular Structure and Function, Springer-Verlag, NY, 1989.
3 D.M. Small (Ed.), The Physical Chemistry of Lipids: From Alkanes to Phospholipids, Handbook of Lipids Research, Vol. 4, Plenum, NY, 1986.
4 D. Chapman, The Structure of Lipids, Methuen, London, 1965.
5 D. Chapman, R.M. Williams and B.D. Ladbrooke, Physical studies of phospholipids VI. Thermotropic and lyotropic mesomorphism of some 1,2-diacyl-phosphatidylcholines (lecithins), Chem. Phys. Lipids 1 (1967) 445–475.
6 D. Chapman, Biological Membranes, Vol. 1, Academic Press, NY, 1968.
7 B.D. Ladbrooke, R.M. Williams and D. Chapman, Studies on lecithin–cholesterol–water interactions by differential scanning calorimetry and X-ray diffraction, Biochim. Biophys. Acta, 150 (1968) 333.
8 B.D. Ladbrooke and D. Chapman, Thermal analysis of lipids, proteins and biological membranes, Chem. Phys. Lipids, 3 (1969) 304–367.
9 D.L. Melchior, F.J. Scavitto, M.T. Walsh and J.M. Steim, Thermal techniques in biomembrane and lipoprotein research, Thermochim. Acta, 18 (1977) 43–71.
10 A.G. Lee, Lipid phase transitions and phase diagrams. I. Lipid phase transitions, Biochim. Biophys. Acta, 472 (1977) 237–281.
11 A.G. Lee, Lipid phase transition and phase diagrams. II. Mixtures involving lipids, Biochim. Biophys. Acta, 472 (1977) 285–344.

12 B.G. Barisas and S.J. Gill, Microcalorimetry of Biological Systems, Annu. Rev. Phys. Chem., 29 (1978) 141–166.
13 S. Mabrey and J.M. Sturtevant, High-sensitivity differential scanning calorimetry in the study of biomembranes and related model systems, in E.D. Korn (Ed.), Methods in Membrane Biology, Vol. 9, Plenum, NY, 1979, pp. 237–274.
14 R.N. McElhaney, The use of differential scanning calorimetry and differential thermal analysis in studies of model and biological membranes, Chem. Phys. Lipids, 30 (1982) 229–259.
15 D. Bach, Calorimetric studies of model and natural biomembranes, in D. Chapman (Ed.), Biomembrane Structure and Function: Topics in Molecular and Structural Biology, Vol. 4, Verlag Chemie, Weinheim, 1984, pp. 1–41.
16 K.M.W. Keough and P.J. Davis, Thermal analysis of membranes, in M.A. Korn and L.A. Manson (Eds.), Membrane Fluidity: Biomembranes, Vol. 12, Plenum, NY, 1986, pp. 55–97.
17 J.W. Donovan, Scanning calorimetry of complex biological structures, Trends Biochem. Sci., 9 (1984) 340–344.
18 B. Maggio, G.D. Fidelio, F.A. Cumar and R.K. Yu, Molecular interactions and thermotropic behavior of glycosphingolipids in model membrane systems, Chem. Phys. Lipids, 42 (1986) 49–63.
19 R.N. McElhaney, Differential scanning calorimetric studies of lipid–protein interactions in model membrane systems, Biochim. Biophys. Acta, 864 (1986) 361–421.
20 C.H. Huang and J.T. Mason, Structure and properties of mixed-chain phospholipid assemblies, Biochim. Biophys. Acta, 864 (1986) 423–470.
21 M.N. Jones, The thermal behaviour of lipid and surfactant systems, in M.N. Jones (Ed.), Biochemical Thermodynamics, 2nd Edn., Elsevier, Amsterdam, 1988, pp. 182–240.
22 J.M. Boggs, Lipid intermolecular hydrogen bonding: influence on structural organization and membrane function, Biochim. Biophys. Acta, 906 (1987) 353–404.
23 A. Blume, Applications of calorimetry to lipid model membranes, in C. Hidalgo (Ed.), Physical Properties of Biological Membranes and Their Functional Implications, Plenum, NY, 1988, pp. 71–121.
24 G. Cevc, Membrane electrostatics, Biochim. Biophys. Acta, 1031 (3) (1990) 311–382.
25 J. Engel and G. Schwarz, Kooperative Konformationsumwandlungen von linearen Biopolymeren, Angew. Chem., 82 (1979) 468–479.
26 H. Träuble, Phasenumwandlungen in Lipiden: Mögliche Schaltprozesse in biologischen Membranen, Naturwissenschaften, 58 (1971) 277–284.
27 J.F. Nagle, Theory of the main lipid bilayer phase transition, Annu. Rev. Phys. Chem., 31 (1980) 157–195.
28 O.G. Mouritsen, Computer studies of phase transitions of critical phenomena, in H. Cabbanes, M. Holt, H.B. Keller, J. Killeen, S.A. Orszag, V.V. Rusanov (Eds.), Springer Series in Computational Physics, Springer-Verlag, Berlin, 1984, pp. 1–200.
29 P.L. Privalov, V.V. Plotnikov and V.V. Filimonov, Precision scanning microcalorimeter for the study of liquids, J. Chem. Thermodyn., 7 (1975) 41–47.
30 S.C. Chen, J.M. Sturtevant and B.J. Gaffney, Scanning calorimetric evidence for a third phase transition in phosphatidylcholine, Proc. Natl. Acad. Sci. U.S.A., 77 (1980) 5060–5063.
31 R.N.A.H. Lewis, N. Mak and R.N. McElhaney, A differential scanning calorimetric study of the thermotropic phase behaviour of model membranes composed of phosphatidylcholines containing linear saturated fatty acyl chains, Biochemistry, 26 (1987) 6118–6126.
32 J.M. Seddon, K. Harlos and D. Marsh, Metastability and polymorphism in the gel and fluid bilayer phases of dilauroylphosphatidylethanolamine, J. Biol. Chem., 258 (1983) 3850–3854.

33 A. Blume, D.M. Rice, R.J. Wittebort and R.G. Griffin, Molecular dynamics and conformation in the gel and liquid-crystalline phases of phosphatidylethanolamine bilayers, Biochemistry, 21 (1982) 6220–6230.
34 D. Marsh, A. Watts and I.C.P. Smith, Dynamic structure and phase behaviour of dimyristoylphosphatidylethanolamine bilayers studied by deuterium nuclear magnetic resonance, Biochemistry, 22 (1983) 3023–3026.
35 P.G. Barton and F.D. Gunstone, Hydrocarbon chain packing and molecular motion in phospholipid bilayers formed from unsaturated lecithins: synthesis and properties of sixteen positional isomers of 1,2-dioctadecenoyl-*sn*-glycerol-3-phosphorylcholine, J. Biol. Chem., 250 (1975) 4470–4476.
36 F.M. Menger, M.G. Wood, Jr., Q.Z. Zhou, H.P. Hopkins and J. Fumero, thermotropic properties of synthetic chain-substituted phosphatidylcholines: effect of substituent size, polarity, number, and location on molecular packing in bilayers, J. Am. Chem. Soc., 110 (1988) 6804–6810.
37 R.N.A.H. Lewis, B.D. Sykes and R.N. McElhaney, Thermotropic phase behavior of model membranes composed of phosphatidylcholines containing cis-monounsaturated acyl chain homologues of oleic acid: differential scanning calorimetric and ^{31}P NMR spectroscopic studies, Biochemistry, 27 (1988) 880–887.
38 J. Shah, P.K. Sripada and G.G. Shipley, Structure and properties of mixed-chain phosphatidylcholine bilayers, Biochemistry, 29 (1990) 4254–4262.
39 P.B. Hitchcock, R. Mason, K.M. Thomas and G.G. Shipley, Structural chemistry of 1,2-dilauroyl-DL-phosphatidylethanolamine: molecular conformation and intermolecular packing of phospholipids, Proc. Natl. Acad. Sci. U.S.A., 71 (1974) 3036–3040.
40 H. Hauser, I. Pascher, R.H. Pearson and S. Sundell, Preferred conformation and molecular packing of phosphatidylethanolamine and phosphatidylcholine, Biochim. Biophys. Acta, 650 (1981) 21–51.
41 A. Blume, K. Habel, T. Frey and A. Finke, DSC-studies of phospholipids with iso-branched and ω-cyclohexane fatty acids, Thermochim. Acta, 114 (1987) 53–58.
42 R.N.A.H. Lewis, D.A. Mannock, R.N. McElhaney, D.C. Turner and S.M. Gruner, Effect of fatty acyl chain length and structure on the lamellar gel to liquid-crystalline and lamellar to reversed hexagonal phase transitions of aqueous phosphatidylethanolamine dispersions, Biochemistry, 28 (1989) 541–548.
43 J.T. Mason and F.A. Stephenson, Thermotropic properties of saturated mixed acyl phosphatidylethanolamines, Biochemistry, 29 (1990) 590–598.
44 J.M. Seddon, G. Cevc and D. Marsh, Calorimetric studies of the gel–fluid (L_β–L_α) and lamellar–inverted hexagonal (L_α–H_{II}) phase transitions in dialkyl- and diacyl-phosphatidylethanolamines, Biochemistry, 22 (1983) 1280–1289.
45 W. Knoll, G. Schmidt and E. Sackmann, Critical demixing in fluid bilayers of phospholipid mixtures: a neutron diffraction study, J. Chem. Phys., 79 (1983) 3439–3442.
46 W. Hübner and A. Blume, ^2H NMR spectroscopic investigations of phospholipid bilayers, Ber. Bunsenges. Phys. Chem., 91 (1987) 1127–1132.
47 P.H. von Dreele, Estimation of lateral species separation from phase transitions in non-ideal two-dimensional lipid mixtures, Biochemistry, 17 (1978) 3939–3943.
48 E. Freire and B. Snyder, Estimation of lateral distribution of molecules in two-component lipid bilayers, Biochemistry, 19 (1980) 88–94.
49 A.G. Lee, Calculation of phase diagrams for non-ideal mixtures of lipids, and a possible non-random distribution of lipids in the liquid-crystalline phase, Biochim. Biophys. Acta, 507 (1978) 433–444.
50 I.P. Sugar and G. Monticelli, Landau-theory of two-component phospholipid bilayers. I. Phosphatidylcholine/phosphatidylethanolamine mixtures, Biophys. Chem., 18 (1983) 281–289.
51 I.P. Sugar and G. Monticelli, Interrelationships between the phase diagrams of the two-component phospholipid bilayers, Biophys. J., 48 (1985) 283–288.

52 H.-D. Dörfler, G. Brezesinski and P. Miethe, Phase diagrams of pseudo-binary phospholipid systems. I. Influence of the chain length differences on the miscibility properties of cephaline/cephaline/water systems, Chem. Phys. Lipids, 48 (1988) 245–254.
53 H.-D. Dörfler, P. Miethe and A. Möps, Phase diagrams of pseudo-binary phospholipid systems. III. Influence of the head group methylation on the miscibility behaviour of *N*-methylated phosphatidylethanolamine mixtures in aqueous dispersions, Chem. Phys. Lipids, 54 (1990) 171–179.
54 E.E. Brumbaugh, M.L. Johnson and C.-H. Huang, Non-linear least squares analysis of phase diagrams for non-ideal binary mixtures of phospholipids, Chem. Phys. Lipids, 52 (1990) 69–78.
55 I.P. Sugar, Cooperativity and classification of phase transitions: application to one- and two-component phospholipid membranes, J. Phys. Chem., 91 (1987) 95–101.
56 E.A. Guggenheim, The theoretical basis for Raoult's law, Trans. Faraday Soc., 33 (1937) 151–159.
57 S. Mabrey and J.M. Sturtevant, Investigation of phase transitions of lipids and lipid mixtures by high sensitivity differential scanning calorimetry, Proc. Natl. Acad. Sci. U.S.A., 73 (1976) 3862–3866.
58 K. Habel, Ph.D. Thesis, University of Freiburg, 1989.
59 T.A. Langworthy, Lipids of bacteria living in extreme environments, in S. Razin, S. Rottem (Eds.), Current Topics in Membranes and Transport, Vol. 17, Membrane Lipids of Prokaryotes, Academic Press, NY, 1982, pp. 45–77.
60 A. Blume, R. Dreher and K. Poralla, The influence of branched-chain and ω-alicyclic fatty acids on the transition temperature of *Bacillus subtilis* lipids, Biochim. Biophys. Acta, 512 (1978) 489–494.
61 R.B. Sisk, Z.-Q. Wang, H.-N. Lin and C.-H. Huang, Mixing behavior of identical molecular weight phosphatidylcholines with various chain-length differences in two-component lamellae, Biophys. J., 58 (1990) 777–783.
62 H. Eibl and A. Blume, The influence of charge on phosphatidic acid bilayer membranes, Biochim. Biophys. Acta, 553 (1979) 467–488.
63 A. Blume and H. Eibl, The influence of charge on bilayer membranes: calorimetric investigations of phosphatidic acid bilayers, Biochim. Biophys. Acta, 558 (1979) 13–21.
64 F. Jähnig, K. Harlos, H. Vogel and H. Eibl, Electrostatic interactions at charged lipid membranes: electrostatically induced tilt, Biochemistry, 18 (1979) 1459–1468.
65 A. Blume and H. Eibl, A calorimetric study of the thermotropic behavior of 1,2-dipentadecylmethylidene phospholipids, Biochim. Biophys. Acta, 640 (1981) 609–618.
66 S.A. Simon, L.J. Lis, J.W. Kauffman and R.C. MacDonald, A calorimetric and monolayer investigation of the influence of ions on the thermodynamic properties of phosphatidylcholine, Biochim. Biophys. Acta, 375 (1975) 317–326.
67 B.Z. Chowdry, G. Lipka, A.W. Dalziel and J.M. Sturtevant, Effect of lanthanum ions on the phase transitions of lecithin bilayers, Biophys. J., 45 (1984) 633–635.
68 T.H. Huang, A. Blume, S.K. Das Gupta and R.G. Griffin, Nuclear magnetic resonance and calorimetric study of the structure, dynamics and phase behavior of uranyl ion/dipalmitoylphosphatidylcholine complexes, Biophys. J., 54 (1988) 173–179.
69 J.M. Boggs and G. Rangaraj, Investigations of the metastable phase behaviour of phosphatidylglycerol with divalent cations by calorimetry and manganese binding measurements, Biochemistry, 22 (1983) 5424–5435.
70 T. Ito and S. Ohnishi, Ca^{2+} induced lateral phase separations in phosphatidic acid–phosphatidylcholine membranes, Biochim. Biophys. Acta, 352 (1974) 29–37.
71 H.J. Galla and E. Sackmann, Chemically induced lipid phase separation in model membranes containing charged lipids: a spin label study, Biochim. Biophys. Acta, 401 (1975) 509–529.
72 R.A. Demel and B. de Kruijff, The function of sterols in membranes, Biochim. Biophys. Acta, 457 (1976) 109–132.

73 P.L. Yeagle, Cholesterol and the cell membrane, Biochim. Biophys. Acta, 822 (1985) 267–287.
74 S. Mabrey, P.L. Mateo and J.M. Sturtevant, High-sensitivity scanning calorimetry study of mixtures of cholesterol with dimyristoyl- and dipalmitoyl-phosphatidylcholines, Biochemistry, 17 (1978) 2464–2468.
75 T.N. Estep, D.B. Mountcastle, R.L. Biltonen and T.E. Thompson, Studies on the anomalous thermotropic behavior of aqueous dispersions of dipalmitoylphosphatidylcholine–cholesterol mixtures, Biochemistry, 17 (1978) 1984–1989.
76 M.R. Vist and J.H. Davis, Phase equilibria of cholesterol/dipalmitoylphosphatidylcholine mixtures: ^{2}H nuclear magnetic resonance and differential scanning calorimetry, Biochemistry, 29 (1990) 451–464.
77 B.R. Lentz, D.A. Barrow and M. Hoechli, Cholesterol–phosphatidylcholine interactions in multilamellar vesicles, Biochemistry, 19 (1980) 1943–1954.
78 K. Mortensen, W. Pfeiffer, E. Sackmann and W. Knoll, Structural properties of a phosphatidylcholine–cholesterol system as studied by small angle neutron scattering: ripple structure and phase diagram, Biochim. Biophys. Acta, 945 (1988) 221–245.
79 I. Hatta and S. Imaizumi, A.C. calorimetric study of phospholipid–cholesterol systems and their structures, Mol. Cryst. Liq. Cryst., 124 (1985) 219–224.
80 R.J. Wittebort, A. Blume, T.H. Huang, S.K. Das Gupta and R.G. Griffin, Carbon-13 nuclear magnetic resonance investigations of phase transitions and phase equilibria in pure and mixed phospholipid bilayers, Biochemistry, 21 (1982) 3481–3502.
81 A. Blume and R.G. Griffin, Carbon-13 and deuterium nuclear magnetic resonance study of the interaction of cholesterol with phosphatidylethanolamine, Biochemistry, 21 (1982) 6230–6242.
82 J.H. Ipsen, G. Karlström, O.G. Mouritsen, H. Wennerström and M.J. Zuckerman, Phase equilibria in phosphatidylcholine–cholesterol systems, Biochim. Biophys. Acta, 905 (1987) 162–172.
83 L. Cruzeiro-Hansen, J.H. Ipsen and O.G. Mouritsen, Intrinsic molecules in lipid membranes change the lipid-domain interfacial area: cholesterol at domain interfaces, Biochim. Biophys. Acta, 979 (1989) 166–176.
84 M.A. Singer and L. Finegold, Cholesterol interacts with all of the lipid in the bilayer membranes: implications for models, Biophys. J., 57 (1990) 153–156.
85 M.A. Singer and L. Finegold, Interaction of cholesterol with saturated phospholipids: role of the C(17) side chain, Chem. Phys. Lipids, 56 (1990) 217–222.
86 A. Blume, Thermotropic behavior of phosphatidylethanolamine–cholesterol and phosphatidylethanolamine–phosphatidylcholine–cholesterol mixtures, Biochemistry, 19 (1980) 4908–4913.
87 W.I. Calhoun and G.G. Shipley, Sphingomyelin–lecithin bilayers and their interactions with cholesterol, Biochemistry, 18 (1979) 1717–1722.
88 S.J. Singer and G.L. Nicolson, The fluid mosaic model of the structure of cell membranes, Science, 175 (1972) 720–731.
89 J.M. Steim, M.E. Tourtelotte, J.C. Reinert, R.N. McElhaney and R.L. Rader, Calorimetric evidence for the liquid-crystalline state of lipids in a biomembrane, Proc. Natl. Acad. Sci. U.S.A., 63 (1969) 104–109.
90 K. Brandenburg and A. Blume, Investigations into the thermotropic phase behaviour of natural membranes extracted from gram-negative bacteria and artificial membrane systems made from lipopolysaccharides and free lipid A, Thermochim. Acta, 119 (1987) 127–142.
91 D. Papahadjopoulos, M. Moscarello, E.H. Eylar and T. Isac, Effects of proteins on thermotropic phase transitions of phospholipid membranes, Biochim. Biophys. Acta, 401 (1975) 317–335.
92 M.R. Morrow, J.C. Huschilt and J.H. Davis, Simultaneous modelling of phase and

calorimetric behaviour in an amphiphilic peptide/phospholipid model membrane, Biochemistry, 24 (1985) 5396–5406.
93 W.K. Surewicz and R.M. Epand, Phospholipid structure determines the effects of peptides on membranes: differential scanning calorimetry studies with pentagastrin-related peptides, Biochim. Biophys. Acta, 856 (1986) 290–300.
94 R.M. Epand and J.M. Sturtevant, A calorimetric study of peptide–phospholipid interactions: the glucagon–dimyristoylphosphatidylcholine complex, Biochemistry, 20 (1981) 4603–4606.
95 W. Curatolo, J.D. Sakura, D.M. Small and G.G. Shipley, Protein–lipid interactions: recombinants of the proteolipid apoprotein of myelin with dimyristoyllecithin, Biochemistry, 16 (1977) 2313–2319.
96 J.M. Boggs, M.A. Moscarello and D. Papahadjopoulos, Phase separation of acidic and neutral phospholipids induced by human myelin basic protein, Biochemistry, 16 (1977) 5420–6526.
97 M. Heyn, A. Blume, M. Rehorek and N. Dencher, Calorimetric and fluorescence depolarization studies on the lipid phase transition of bacteriorhodopsin–dimyristoylphosphatidylcholine vesicles, Biochemistry, 20 (1981) 7109–7115.
98 A. Alonso, C.J. Restall, M. Turner, J.C. Gomez-Fernandez, F.M. Goni and D. Chapman, Protein–lipid interactions and differential scanning calorimetric studies of bacteriorhodopsin reconstituted lipid–water systems, Biochim. Biophys. Acta, 689 (1982) 283–289.
99 B.K. Semin, M. Saraste and M. Wikström, Calorimetric studies of cytochrome oxidase–phospholipid interactions, Biochim. Biophys. Acta, 769 (1984) 15–22.
100 C.A. Yu, S.H. Gwak and L. Yu, Studies on protein–lipid interactions in cytochrome *c* oxidase by differential scanning calorimetry, Biochim. Biophys. Acta, 812 (1985) 656–664.
101 J.B. Massey, A.M. Gotto, Jr. and H.J. Pownall, Thermodynamics of lipid–protein interactions: interaction of apolipoprotein A-II from human plasma high-density lipoproteins with dimyristoylphosphatidylcholine, Biochemistry, 20 (1981) 1575–1584.
102 C.-A. Yu, J.R. Steidl and L. Yu, Microcalorimetric studies of the interactions between cytochromes *c* and c_1 and of their interactions with phospholipids, Biochim. Biophys. Acta, 736 (1983) 226–234.
103 J.C. Gomez-Fernandez, F.M. Goni, D. Bach, C. Restall and D. Chapman, Protein–lipid interactions: a study of $(Ca^{2+}$–$Mg^{2+})$ATPase reconstituted with synthetic phospholipids, FEBS Lett., 98 (1979) 224–228.
104 C. Mollay, Effect of melittin and melittin fragments on the thermotropic phase transition of dipalmitoyllecithin and on the amount of lipid-bound water, FEBS Lett., 64 (1976) 65–68.
105 E. Bernard, J.F. Faucon and J. Dufourcq, Phase separations induced by melittin in negatively-charged phospholipid bilayers as detected by fluorescence polarization and differential scanning calorimetry, Biochim. Biophys. Acta, 688 (1982) 152–162.
106 T.C. Terwilliger, L. Weissman and D. Eisenberg, The structure of melittin in the form I crystals and its implication for melittin's lytic and surface activities, Biophys. J., 37 (1982) 353–361.
107 E.J. Dufourc, J.F. Faucon, G. Fourche, J. Dufourcq, T. Gulik-Grzywicki and M. le Maire, Reversible disc-to-vesicle transition of melittin–DPPC complexes triggered by the phospholipid acyl chain melting, FEBS Lett., 201 (1986) 205–209.
108 D.A. Wilkinson and J.F. Nagle, Specific heats of lipid dispersions in single phase regions, Biochim. Biophys. Acta, 688 (1982) 107–115.
109 A. Blume, Apparent molar heat capacities of phospholipids in aqueous dispersion. Effects of chain length and head group structure, Biochemistry, 22 (1983) 5436–5442.
110 P.I. Bendzko, W.A. Pfeil, P.L. Privalov and E.I. Tiktopulo, Temperature-induced phase

transitions in proteins and lipids: volume and heat capacity effects, Biophys. Chem., 29 (1988) 301–307.
111 P.L. Privalov and N.N. Khechinashvili, Thermodynamic approach to the problem of stabilization of globular protein structure: a calorimetric study, J. Mol. Biol., 86 (1974) 665–684.
112 A. Chen and I. Wadsö, Simultaneous determination of ΔG, ΔH, and ΔS by an automatic microcalorimetric titration technique: application to protein ligand binding, J. Biochem. Biophys. Methods, 6 (1982) 307–316.
113 T. Wiseman, S. Williston, J.F. Brandts and L.-N. Lin, Rapid measurement of binding constants and heats of binding using a new titration calorimeter, Anal. Biochem., 179 (1989) 131–137.
114 H. Träuble, M. Teubner, P. Woolley and H. Eibl, Electrostatic interactions at charged lipid membranes. I. Effects of pH and univalent cations on membrane structure, Biophys. Chem., 4 (1976) 319–342.
115 F. Jähnig, Electrostatic free energy and shift of the phase transition for charged lipid membranes, Biophys. Chem., 4 (1976) 309–318.
116 F. Jähnig, Thermodynamics and kinetics of protein incorporation into membranes, Proc. Natl. Acad. Sci. U.S.A., 80 (1983) 3691–3695.
117 (a) W. Hübner, Ph.D. Thesis, University of Freiburg, 1988.
(b) W. Hübner and A. Blume, unpublished results, 1988.
118 A. Blume, in preparation.
119 A. Blume, unpublished results, 1989.
120 A. Blume and J. Tuchtenhagen, Biochemistry, submitted for publication.
121 J. Tuchtenhagen, Diploma Thesis, University of Kaiserlautern, 1990.